
Superluminous supernovae

Takashi J. Moriya* · Elena I. Sorokina ·
Roger A. Chevalier

Received: 25 December 2017 / Accepted: 5 March 2018

Abstract Superluminous supernovae are a new class of supernovae that were recognized about a decade ago. Both observational and theoretical progress has been significant in the last decade. In this review, we first briefly summarize the observational properties of superluminous supernovae. We then introduce the three major suggested luminosity sources to explain the huge luminosities of superluminous supernovae, i.e., the nuclear decay of ^{56}Ni , the interaction between supernova ejecta and dense circumstellar media, and the spin down of magnetars. We compare these models and discuss their strengths and weaknesses.

Keywords supernovae · superluminous supernovae · massive stars

1 Introduction

Superluminous supernovae (SLSNe) are supernovae (SNe) that become more luminous than ~ -21 mag in optical. They are more than 1 mag more luminous than broad-line Type Ic SNe, or the so-called “hypernovae,”

* NAOJ Fellow

T. J. Moriya
Division of Theoretical Astronomy, National Astronomical Observatory of Japan,
National Institutes of Natural Sciences, 2-21-1 Osawa, Mitaka, Tokyo 181-8588,
Japan
E-mail: takashi.moriya@nao.ac.jp

E. I. Sorokina
Sternberg Astronomical Institute, M.V. Lomonosov Moscow State University, Uni-
versitetski pr. 13, 119234 Moscow, Russia
E-mail: sorokina@sai.msu.su

R. A. Chevalier
Department of Astronomy, University of Virginia, P.O. Box 400325, Charlottesville,
VA 22904-4325, USA
E-mail: rac5x@virginia.edu

which have kinetic energy of more than $\sim 10^{52}$ erg and are the most luminous among the classical core-collapse SNe. The first glimpse of their existence was in SN 1999as (Knop et al 1999). Other SLSNe, such as SCP06F6 (Barbary et al 2009), were subsequently discovered. However, their nature was not clarified until SLSNe started to be discovered regularly with unbiased transient surveys such as that conducted by the ROTSE-IIIb telescope (Quimby 2006). Nowadays, SLSNe are discovered even at redshifts around 2 and beyond (Cooke et al 2012, Pan et al 2017, Smith et al 2018, Moriya et al 2018, Curtin et al 2018), and they are becoming an important probe of, e.g., massive star formation in the high-redshift universe. They may be eventually applicable to cosmology like Type Ia SNe (Quimby et al 2013, Inserra and Smartt 2014, Inserra et al 2018a, Scovaccicchi et al 2016, Wei et al 2015). They can also be a back light source to study interstellar media (Berger et al 2012).

This review mainly focuses on theoretical aspects of the energy sources of SLSNe. Three energy sources are mainly suggested to account for the huge luminosities of SLSNe, i.e., ^{56}Ni decay (Section 3), interaction between ejecta and dense circumstellar media (CSM, Section 4), and magnetar spin-down (Section 5). We start this review with a brief summary of the observational properties in Section 2 and then discuss the theoretical aspects of the power sources. We compare three models in Section 6. For a review of observational aspects of SLSNe, see, e.g., Gal-Yam (2012) and Howell (2017). Observational data on SLSNe are now available at <https://slsn.info/>, which is maintained by T.-W. Chen.

2 Observational properties

Broadly speaking, SLSNe can be classified in two different spectral types; those with narrow hydrogen emission lines (Type IIn, e.g., Smith et al 2010) and those without (e.g., Quimby et al 2011). Most of SLSNe without the narrow hydrogen emission lines are classified as Type Ic and we simply call them SLSNe Ic. However, some SLSNe show broad hydrogen lines (e.g., Inserra et al 2018b) and there exist some SLSNe that are initially Type Ic but start to show hydrogen emissions about 1 year after the luminosity peak (Yan et al 2015, 2017a). We introduce Type IIn SLSNe in Section 2.1 and then the other SLSNe in Section 2.2. We discuss the event rates of SLSNe in Section 2.3 and their environment in Section 2.4.

2.1 Type IIn SLSNe

SLSNe IIn are characterized by narrow emission lines (Fig. 1). Narrow hydrogen emission lines are particularly strong. The spectral characteristics of SLSNe IIn are similar to those of less luminous SNe IIn. Therefore, they are believed to be extreme cases of SNe IIn where their luminosities are mainly powered by the interaction between ejecta and dense CSM (Section 4). SN 2006gy is the closest and the best observed SN in this class

(e.g., Ofek et al 2007, Smith et al 2007, 2008b, 2010, Kawabata et al 2009, Agnoletto et al 2009, Miller et al 2010).

Although the light curves (LCs) of SLSNe IIn share the characteristics that they become extremely luminous, their LC shapes are diverse (Fig. 1). SN 2008fz (Drake et al 2010) and SN 2006gy (Smith et al 2007) have broad round LCs lasting for more than 100 days while SN 2003ma (Rest et al 2011) has a short round phase followed by a long phase of constant luminosity. The LCs of less luminous Type IIn SNe like SN 2006tf (Smith et al 2008a) and SN 2010jl (Zhang et al 2012, Fransson et al 2014) often decline with a power law. These diversities are likely to originate from the diversity in the CSM related to the diversity in the mass loss processes of the progenitors.

It is not yet clear if SLSNe IIn are just the most luminous end of a SN IIn luminosity function or SLSNe IIn make a separate population of their own (e.g., Richardson et al 2014). There exist several SNe IIn whose peak luminosity is between ~ -20 mag and ~ -21 mag. These luminous populations can be observed more easily but there do not exist many SNe IIn with which we can make a volume-limited sample because of their small event rate. The most luminous SLSN IIn reported so far is CSS100217:102913+404220 reaching -23 mag in the optical at the LC peak (Drake et al 2011, see also Kankare et al 2017). Although CSS100217:102913+404220 and other similar objects are suggested to originate from stellar explosions, they appear at the centers of galaxies with active galactic nuclei and their stellar explosion origin is doubted (e.g., Blanchard et al 2017, Moriya et al 2017b). The most luminous published SLSN IIn without a clear association with an active galactic nucleus is SN 2008fz (Drake et al 2010).

2.2 Type Ic SLSNe

SLSNe Ic, which are often simply called SLSNe I, are SLSNe without hydrogen spectral features around the time of the luminosity peak (e.g., Quimby et al 2011). Fig. 2 shows LCs and spectra of SLSNe Ic. The peak optical magnitudes of SLSNe Ic are typically between ~ -21 mag and -22 mag (e.g., Nicholl et al 2015a, De Cia et al 2017, Lunnan et al 2018). The distribution of their peak bolometric magnitudes derived from optical LCs peaks at -20.7 mag with a small dispersion of 0.5 mag (Nicholl et al 2015a). The luminosity function of Type Ibc SNe peaks at around -18 mag with a dispersion of more than 0.5 mag (Drout et al 2011, Taddia et al 2015, Lyman et al 2016). Therefore, there may exist a gap in the hydrogen-poor SN luminosity function between ~ -20 mag and ~ -21 mag, where a small number of Type Ic BL supernovae and some gap transients exist (Arcavi et al 2016, Roy et al 2016). The rise times of SLSNe Ic have a diversity, ranging from $\simeq 20$ days (PTF11rks, Inserra et al 2013) to more than 125 days (PS1-14bj, Lunnan et al 2016). However, their LC decline rates may have two distinct classes: rapidly-declining ones and slowly-declining ones (e.g., Nicholl et al 2015a). The LC decline rates of slowly-declining SLSNe Ic are often consistent with the nuclear decay rate of ^{56}Co (e.g., Gal-Yam et al 2009, Inserra et al 2017) and they are sometimes referred as

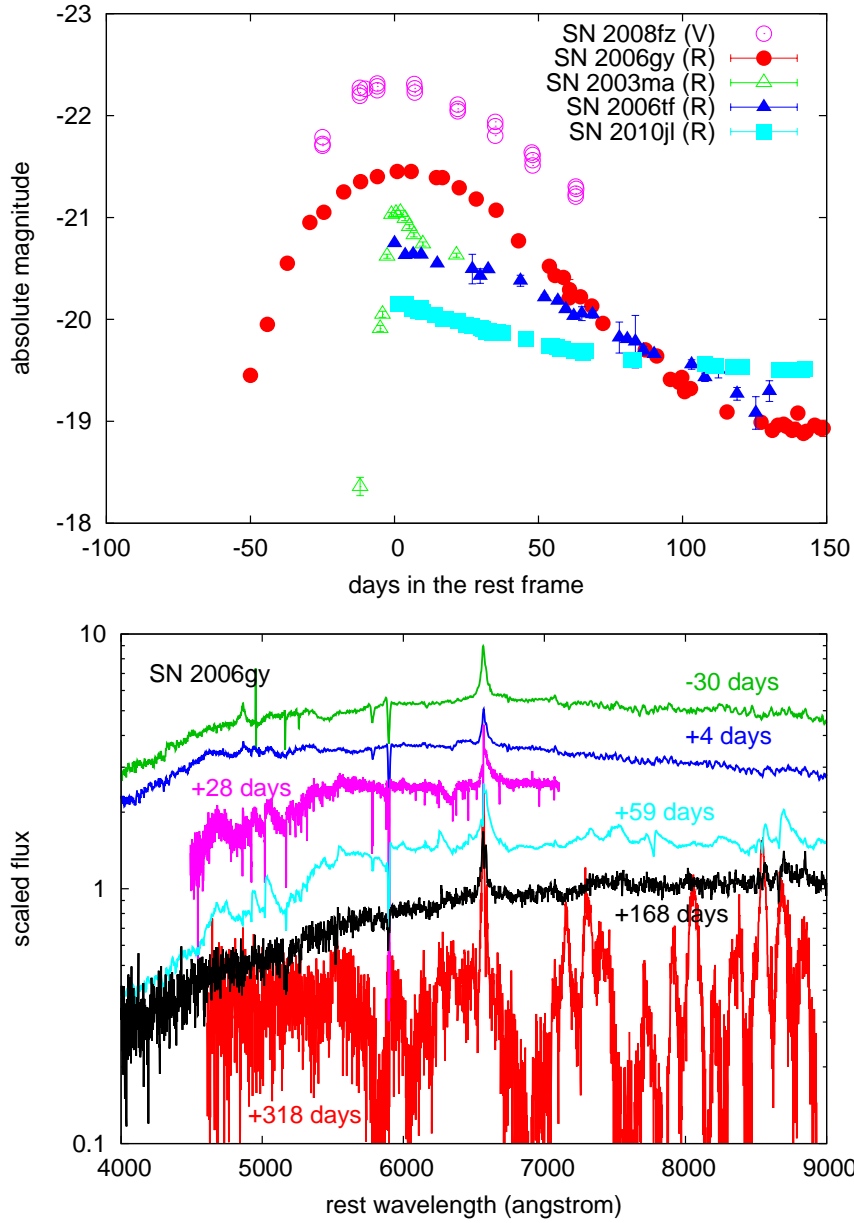


Fig. 1 *Top*: LC diversities in Type IIIn SLSNe. The SN names and observed bands are indicated in the figure. The data sources are: Drake et al (2010) (SN 2008fz), Smith et al (2007) (SN 2006gy), Rest et al (2011) (SN 2003ma), Smith et al (2008a) (SN 2006tf), and Zhang et al (2012) (SN 2010jl). *Bottom*: Spectroscopic evolution of SLSN II_n 2006gy (e.g., Smith et al 2010, Kawabata et al 2009). The dates are relative to the luminosity peak in the *R* band in the rest frame.

SLSN R, with “R” for radioactive decay (Gal-Yam 2012). However, whether they are powered by nuclear decay or not cannot be judged solely based on the LCs (e.g., Moriya et al 2017a). The slowly-declining SLSNe Ic may tend to be intrinsically more luminous than rapidly-declining SLSNe Ic, which may enable us to use SLSNe Ic as a distance indicator like Type Ia SNe (Inserra and Smartt 2014, but see also Quimby et al 2013).

The LCs of SLSNe Ic have a distinguishing feature at the very beginning. They often show a precursor before the main luminosity increase (e.g., Nicholl et al 2015b, Smith et al 2016, Vreeswijk et al 2017). The possible existence of the precursor was first found in SN 2006oz (Leloudas et al 2012) and it was systematically studied by Nicholl and Smartt (2016). The precursor lasts for about 5 – 10 days and its magnitude is around -20 mag. Its blackbody temperature is around 30,000 K (Nicholl and Smartt 2016). The precursor is followed by a fading lasting for about 5 days and the luminosity is about 1 mag fainter than the precursor luminosity in this period. Then, the LC starts to rise again to be a SLSN.

LC behaviors of slowly-declining SLSNe Ic during the fading phase after the LC peak have been intensively studied by Inserra et al (2017). The LCs show fluctuations that may originate from the interaction with the CSM. The LC decline rates are consistent with that of the ^{56}Co decay at first, but tend to decline faster after a few hundred days after the LC peak.

The early-time spectra of SLSNe Ic at around the luminosity peak are characterized by a series of broad carbon and oxygen features (Quimby et al 2011, 2018, Chomiuk et al 2011, Howell et al 2013, Nicholl et al 2014, 2016b, Yan et al 2017c,b, Liu et al 2017b). The blackbody temperature is around 15,000 K at these epochs, but non-thermal excitations play essential roles in forming the spectral features (e.g., Mazzali et al 2016). Photospheric velocities measured by using Fe II $\lambda 5169$ are typically around 12,000 km s $^{-1}$ and they do not evolve fast (e.g., Nicholl et al 2015a). It is suggested that the existence of helium is required for the line formation (Mazzali et al 2016) and a helium line may have been observed in SN 2012il (Inserra et al 2013). At later phases, the spectra often start to be similar to those of broad-line Type Ic SNe (Pastorello et al 2010, Nicholl et al 2016a). In addition, there are several SLSNe Ic that do not show hydrogen features near the LC peak but hydrogen emission lines start to appear about 1 year after the LC peak (Yan et al 2015, 2017a). The late-phase hydrogen emissions have been suggested to originate from a detached hydrogen-rich circumstellar shell (Yan et al 2015, 2017a) or matter stripped from the progenitor’s hydrogen-rich companion star (Moriya et al 2015).

There are a few SLSNe in which broad hydrogen features are observed (Gezari et al 2009, Miller et al 2009, Inserra et al 2018b). They usually do not show narrow features in spectra like SLSNe IIn at early times. Therefore, their powering source may be related to SLSNe Ic. However, their spectra start to show possible signatures of the interaction in the late phase and some luminosity contributions from the interaction may exist after around 1 year since the LC peak. The SLSN CSS121015:004244+132827 showed both broad and narrow hydrogen features from early times (Benetti et al 2014).

Polarization of SLSNe Ic was measured in three objects: LSQ14mo, SN 2015bn, and SN 2017egm. The first attempt was made for LSQ14mo. Leloudas et al (2015a) measured photometric polarization in the V band for 5 epochs and they did not detect clear polarization signatures. SN 2015bn appeared closer and both imaging and spectroscopic polarizations were measured for several epochs (Leloudas et al 2017, Inserra et al 2016). Aspherical shapes may be required to explain the polarization features. SN 2017egm is the closest SLSN Ic and a spectropolarimetry observation was reported (Bose et al 2018). Polarization of about 0.5% without a strong dependence on wavelength is observed, indicating a modest departure from spherical symmetry. More observations are needed to obtain a systematic view of the asphericity in SLSNe Ic. Polarization of one SLSN II with broad hydrogen features is observed but a meaningful constraint on its shape could not be made (Inserra et al 2018b).

SLSNe Ic are also actively observed in X-rays. SCP06F6 is the first SLSN Ic with a possible detection of X-rays (Gänsicke et al 2009, Levan et al 2013). It was detected in X-rays (0.1–2 keV) by the *XMM-Newton* satellite. The X-ray luminosity reached $\sim 10^{45}$ erg s $^{-1}$ in one epoch and then it was not detected any more. Another case is PTF12dam (Margutti et al 2017). It was detected by *Chandra* at 0.5–2 keV in a similar epoch to SCP06F6 but its luminosity is $\sim 10^{40}$ erg s $^{-1}$ and is 5 orders of magnitude below that of SCP06F6. The X-ray luminosity at the location of PTF12dam is consistent with that expected from the underlying star-formation activities at the SN location and the X-rays may not originate from PTF12dam itself. X-ray observations in many other SLSNe Ic have been performed but SCP06F6 and PTF12dam are the only cases with X-ray detections (Margutti et al 2017). No radio emission is observed in SLSNe so far (Coppejans et al 2017).

Gamma-ray bursts (GRBs) are often associated with Type Ic-BL SNe. It is interesting to note that SLSNe Ic have spectra similar to SNe Ic-BL at late phases (e.g., Pastorello et al 2010, Nicholl et al 2016a). In addition, SN 2011kl, which was associated with an ultra-long GRB111209A, had a LC peak at -20 mag and it was much more luminous than SNe usually associated with GRBs (Greiner et al 2015). Although SN 2011kl was not as luminous as SLSNe and its spectroscopic features, which are overall featureless, do not appear to be similar to SLSNe Ic, some GRBs may be related to SLSNe. Yu and Li (2017) speculate that LC modulations in SN 2015bn may be related to flare activity of GRBs. Similarities in GRBs and SLSNe are also suggested in their host environment which will be discussed in a following section.

The most luminous SLSN Ic reported so far is ASASSN-15lh, which reached about -23.5 mag (Dong et al 2016). However, it appeared at the center of the host galaxy and its origin is questioned (Leloudas et al 2016). Its host galaxy is massive and metal-rich and, therefore, is peculiar if it is actually a SLSN Ic (e.g., Leloudas et al 2016). Except for ASASSN-15lh, the most luminous SLSNe Ic reach $-22.5 \sim -23$ mag in optical (e.g., PTF13ajg, Vreeswijk et al 2014).

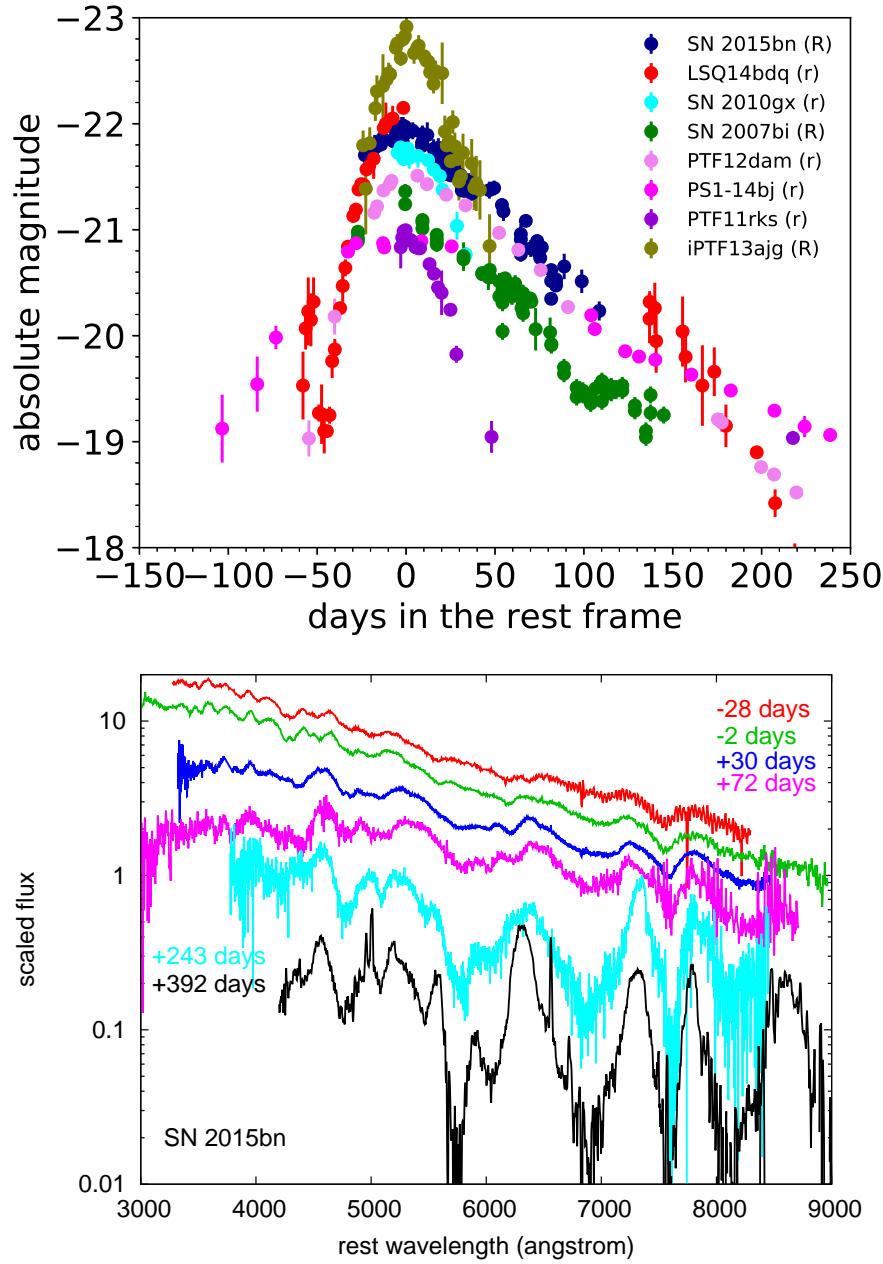


Fig. 2 *Top:* LC diversities in Type Ic SLSNe. The SN names and observed bands are indicated in the figure. The data sources are: Nicholl et al (2016b) (SN 2015bn), Nicholl et al (2015b) (LSQ14bdq), Pastorello et al (2010) (SN 2010gx), Gal-Yam et al (2009) (SN 2007bi), Lunnan et al (2016) (PS1-14bj), Inserra et al (2013) (PTF11rks), and Vreeswijk et al (2014) (iPTF13ajg). *Bottom:* Spectroscopic evolution of SLSN Ic 2015bn (Nicholl et al 2016b,a). The dates are relative to the optical luminosity peak in the rest frame.

2.3 Event rates

Quimby et al (2013) calculate the rates of SLSNe at $z \sim 0.2$. They find a total SLSN rate of $199_{-86}^{+137} \text{ Gpc}^{-3} \text{ yr}^{-1} h_{71}^3$, where h_{71} is the Hubble constant scaled with $71 \text{ km s}^{-1} \text{ Mpc}^{-1}$. They estimate a SLSN II rate of $151_{-82}^{+151} \text{ Gpc}^{-3} \text{ yr}^{-1} h_{71}^3$. Their SLSN II sample consists of SLSNe IIn, with the exception of SN 2008es. The rate of SLSNe Ic is estimated to be $32_{-26}^{+77} \text{ Gpc}^{-3} \text{ yr}^{-1} h_{71}^3$. Because the core-collapse SN rate at $z \sim 0.2$ is $\sim 10^5 \text{ Gpc}^{-3} \text{ yr}^{-1}$ (Madau and Dickinson 2014), the fraction of SLSNe to core-collapse SNe are estimated to be $\sim 10^{-3}$. The total SLSN rate is similar to the long GRB rate (e.g., Soderberg et al 2006) and the SLSN Ic rate may be about 10% of the long GRB rate.

There are two works deriving the SLSN Ic rate at $z \sim 1$. The first work is by McCrum et al (2015) who use a SN sample from the Pan-STARRS survey to derive a relative fraction of SLSNe Ic to core-collapse SNe. They found only $\sim 10^{-5}$ of core-collapse SNe are SLSNe Ic at $z \sim 1$, which is roughly a factor of 10 smaller than the rate at $z \sim 0.2$. The subsequent work by Prajs et al (2017) measured the SLSN Ic rate at $z \sim 1$ based on the SLSN Ic samples from the Supernova Legacy Survey. The survey has two spectroscopically confirmed SLSNe Ic at $z = 1.50$ and 1.59 and one additional SLSN Ic candidate at $z = 0.76$ which is found by fitting the LCs found in the survey. The three SLSNe Ic in the survey give a SLSN Ic rate of $91_{-36}^{+76} \text{ Gpc}^{-3} \text{ yr}^{-1} h_{70}^3$ at $z \sim 1$. This rate is equivalent to $\sim 10^{-4}$ of the core-collapse rate at $z \sim 1$ and an order of magnitude higher than that estimated by McCrum et al (2015).

Cooke et al (2012) reported two SLSNe at $z = 2.05$ and $z = 3.90$. Although their spectral types are not clear, the detection of two SLSNe in their survey very roughly corresponds to the SLSN rate of $\sim 400 \text{ Gpc}^{-3} \text{ yr}^{-1} h_{70}^3$ at $z = 2 - 4$. The increase in the SLSN rate is still consistent with that expected from the increase in the cosmic star-formation rate and it is still not clear if the intrinsic SLSN frequency increases at high redshifts (see also a recent estimate by Moriya et al 2018).

2.4 Environments

The host environments of SLSNe have been studied extensively. SLSNe IIn are known to come from a broad range of metallicities (Neill et al 2011, Perley et al 2016, Schulze et al 2018, Angus et al 2016), while SLSNe Ic only come from metal-poor environments (e.g., Schulze et al 2018, Chen et al 2017c, 2015, 2013, Leloudas et al 2015b, Perley et al 2016, Vreeswijk et al 2014, Lunnan et al 2016). There is likely a suppression of SLSNe Ic above around the half-solar metallicity environment (Perley et al 2016, Chen et al 2017c, Schulze et al 2018). SLSNe Ic also tend to come from star-bursting galaxies with high specific star-formation rates (e.g., Schulze et al 2018). This tendency can be explained if their progenitors are very massive stars (e.g., Thöne et al 2015, Leloudas et al 2015b), but this interpretation is also questioned (e.g., Perley et al 2016). SLSNe Ic are often found in interacting

galaxies where the star formation can be triggered by the interaction (e.g., Chen et al 2017a, Cikota et al 2017). SLSNe Ic may prefer metal-poorer environments than long GRBs (e.g., Schulze et al 2018). However, the differences between SLSNe Ic and long GRB host environments are not yet clear (e.g., Lunnan et al 2014, 2015, Angus et al 2016, Japelj et al 2016).

A SLSN Ic SN 2017egm has appeared in a nearby spiral galaxy that has a high metallicity (Bose et al 2018, Nicholl et al 2017a) but the SN location itself may have low metallicity (Izzo et al 2018, but see also Chen et al 2017b).

An interesting relation between the host metallicities and the spin periods of magnetars required to fit the LCs of SLSNe Ic has been suggested by Chen et al (2017c). This relation may simply come from the relation between the host metallicities and total radiated energy in SLSNe Ic, because the spin periods in the magnetar model represent the total available energy to power SLSNe (Section 5). The suggested relation is still based on a small number of SLSNe Ic and it needs to be studied more. Recent follow-up studies based on larger SLSN samples infer that the relation may not be as strong as originally suggested (Nicholl et al 2017b, De Cia et al 2017).

3 ^{56}Ni -powered models

The standard source of early luminosity in SNe is the nuclear decay of ^{56}Ni . The simplest approach to explain the huge luminosities of SLSNe is to increase the amount of ^{56}Ni . ^{56}Ni decays to ^{56}Co with a decay time of 8.76 ± 0.01 days (da Cruz et al 1992) and then ^{56}Co decays to ^{56}Fe with a decay time of 111.42 ± 0.04 days (Funck et al 1992). The total available energy from the nuclear decay is

$$\left[6.48 \exp\left(-\frac{t}{8.76 \text{ days}}\right) + 1.44 \exp\left(-\frac{t}{111.42 \text{ days}}\right) \right] \frac{M_{^{56}\text{Ni}}}{M_{\odot}} 10^{43} \text{ erg s}^{-1}, \quad (1)$$

where $M_{^{56}\text{Ni}}$ is the total mass of ^{56}Ni available at the beginning (Nadyozhin 1994, but updated based on <http://www.nndc.bnl.gov/chart>). However, all the available energy from the decay is not necessarily absorbed by the SN ejecta to heat them up. All the decay energy of ^{56}Ni and about 97% of the decay energy of ^{56}Co are released in the form of γ -rays. The released γ -rays travel in the ejecta and some fraction is absorbed by the ejecta and heats them up. The effective γ -ray opacity is $0.027 \text{ cm}^2 \text{ g}^{-1}$ (Axelrod 1980). The remaining 3% of the ^{56}Co decay energy is released as positrons that can be all absorbed *in situ* by the ejecta to heat them up. During the early phases when the ejecta are dense, most γ -rays can be absorbed. However, in the nebular phases when the ejecta are optically thin, a proper treatment of the γ -ray transport is needed to estimate the expected luminosity. Because heating by the ^{56}Ni decay is a standard way to power SNe, we refer to a standard text such as Arnett (1996) for further details of the SN properties powered by ^{56}Ni decay.

The required ^{56}Ni masses to explain the peak luminosity of SLSNe are $5 - 20 M_{\odot}$ (e.g., Nicholl et al 2015a). There are several suggested ways to make such a large amount of ^{56}Ni . One is the very energetic explosions of massive stars. Umeda and Nomoto (2008) investigated the explosive nucleosynthesis of very massive stars up to the zero-age main-sequence (ZAMS) mass of $100 M_{\odot}$ with $Z_{\odot}/200$. They show that more than $5 M_{\odot}$ of ^{56}Ni can be produced in massive cores if the explosion energy exceeds 10^{52} erg. To produce more than $10 M_{\odot}$ of ^{56}Ni , which is often required to reproduce the SLSN LCs, an unrealistically high explosion energy of 10^{53} erg is required. Relatively faint SLSNe requiring $\sim 5 M_{\odot}$ of ^{56}Ni , like SN 2007bi, may be explained by the energetic core-collapse explosions of very massive stars (Young et al 2010, Moriya et al 2010).

A promising mechanism to synthesize more than $10 M_{\odot}$ of ^{56}Ni in massive stars is through pair-instability (e.g., Rakavy and Shaviv 1967, Barkat et al 1967). If a star has a core that is massive enough, photons in the stellar core can be efficiently converted to electron and positron pairs and the center of the star can suffer a strong reduction in radiative pressure supporting the massive core. The reduction of the pressure support triggers the contraction of the massive core by making the adiabatic index below $4/3$ and leads to explosive carbon and oxygen burning. If the energy released by the explosive nuclear burning is enough to unbind the whole star, it can explode without leaving any compact remnant. This kind of explosion is called pair-instability SN (PISN). The amount of ^{56}Ni produced in PISNe strongly depends on the core mass of the progenitor and it ranges from almost zero to $\sim 50 M_{\odot}$ (e.g., Heger and Woosley 2002, Takahashi et al 2016). PISNe can occur if helium cores of massive stars are between $\sim 65 M_{\odot}$ and $\sim 135 M_{\odot}$ which corresponds to ZAMS masses between $\sim 150 M_{\odot}$ and $\sim 250 M_{\odot}$ at zero metallicity (e.g., Heger and Woosley 2002). The ZAMS mass can be as low as $65 M_{\odot}$ if massive stars rotate rapidly (e.g., Chatzopoulos and Wheeler 2012, Yusof et al 2013). The rapid rotation also helps PISN progenitors to remove their hydrogen through quasi-chemically homogeneous evolution (e.g., Yoon et al 2012). It is interesting to note that most PISN candidates are hydrogen-free SLSNe (but see Terreran et al 2017), although hydrogen-rich PISNe can also be very luminous (e.g., Kasen et al 2011). The surface instability of red supergiant PISN progenitors can also help reduce the amount of hydrogen in their explosions (Moriya and Langer 2015). PISNe are considered to exist in environments with metallicities less than $\sim Z_{\odot}/3$ (e.g., Langer et al 2007), but they may exist even in a solar-metallicity environment if magnetic fields of massive stars can suppress their mass loss (Georgy et al 2017).

Predicted LCs of PISNe (e.g., Scannapieco et al 2005, Kasen et al 2011, Dessart et al 2013, Whalen et al 2014, Kozyreva et al 2014, Chatzopoulos et al 2015) are roughly consistent with those of slowly-declining SLSNe I whose late-phase decline rates are consistent with the ^{56}Co nuclear decay rate. PISNe tend to have large rise times compared to SLSNe I but some PISN models are consistent with the relatively short rise times of SLSNe Ic (e.g., Kozyreva et al 2017). The internal mixing of PISNe can help reduce their rise times as well (e.g., Kozyreva and Blinnikov 2015) but multidimensional

simulations of PISN explosions generally do not find strong mixing in them (Joggerst and Whalen 2011, Chen et al 2014, Gilmer et al 2017). Crucial issues of PISN models for SLSNe Ic are in their spectroscopic properties. Although PISNe produce a huge amount of ^{56}Ni , it is not sufficient to heat the massive core as much as observed (e.g., Dessart et al 2012). The production of a large amount of ^{56}Ni also leads to the existence of a large amount of Fe-group elements in the ejecta. The absorptions and emissions by the Fe-group elements results in much redder spectra than those observed in SLSN Ic (e.g., Dessart et al 2012, Jerkstrand et al 2016).

Finally, we summarize pros and cons of the ^{56}Ni -powered models.

Pros:

- ^{56}Ni power can naturally explain the decay rate of slowly declining SLSNe Ic.

Cons:

- ^{56}Ni power cannot explain the rapidly declining SLSNe Ic. A different model must be invoked for the rapidly declining SLSNe Ic.
- Spectra of SLSNe Ic do not match those predicted for ^{56}Ni -powered SNe.

4 Interaction-powered models

Interaction of the gas ejected during a SN explosion with an ambient medium is a process that happens quite often at different stages of SN evolution. Interaction leads to shock wave formation, and shocks very efficiently transform the kinetic energy to thermal energy, which can be then radiated at different wavelengths (Chevalier and Fransson 2003). The stage of SN evolution at which significant interaction starts depends on the density of the CSM. If the ejecta expand into low density material, the interaction becomes important at the SN remnant stage, a few tens, hundreds, or even thousands of years after the SN explosion. Up to this age, the ejecta are cold and faint, but the shock interaction with the surrounding material heats it up again (Reynolds 2016). In the case of a dense CSM, the interaction occurs already on the SN stage (e.g., for SNe of Type II_n, see Chandra 2018). The SN becomes more luminous than a normal one exploded in lower density surroundings.

In the case of SLSNe, the radiation energy emitted during the first few months after the explosion is of the order of 10^{50} – 10^{51} ergs (Quimby et al 2011). The kinetic energy of a standard SN explosion is also $\sim 10^{51}$ ergs. Naked SNe preserve almost all their kinetic energy until the remnant stage, when a sufficient amount of ambient mass (comparable to the ejecta mass) is swept up, and the interaction becomes important. If the ambient mass is concentrated close to the exploding star, the interaction starts from the very beginning and there is a good chance to transform the kinetic energy of the ejecta to radiation during the first months, exactly as it is needed to produce a SLSN event.

In this Section we first make crude estimates of some parameters of the explosion in order to understand what kind of structure can produce such

a powerful event as a SLSN in the CSM interaction scenario (Sect. 4.1). Then we briefly discuss how the shock wave propagates through the dense extended CSM (Sect. 4.2). After that we describe analytical and numerical models for the SLSN light curves that originate from ejecta–CSM interaction and discuss the progenitors that are able to provide the required CSM structure (Sect. 4.3). Finally, we list pros and cons of the CSM interaction scenario for SLSNe (Sect. 4.4).

4.1 Estimates of model parameters

Mass ratio $m_{\text{ej}}/m_{\text{CSM}}$ needed for SLSNe. In the CSM interaction scenario for SLSNe, the expanding ejecta collide with the CS envelope that can be static or expanding. Let us consider for simplicity an inelastic collision of two blobs of matter. The first one, which represents the ejecta, has mass m_1 and momentum \mathbf{p}_1 . Its kinetic energy is

$$E_{\text{init}} = \frac{\mathbf{p}_1^2}{2m_1}. \quad (2)$$

It collides with another blob with mass m_2 and, for now, we suppose its momentum to be zero. The final energy of two merged blobs in a fully inelastic collision is

$$E_{\text{fin}} = \frac{\mathbf{p}_1^2}{2(m_1 + m_2)}. \quad (3)$$

The momentum is conserved, but the energy $E_{\text{init}} - E_{\text{fin}}$ is radiated away, since $E_{\text{fin}} < E_{\text{init}}$. If $m_2 \ll m_1$ then only a tiny fraction of E_{init} is radiated, but if $m_2 \gg m_1$ then $E_{\text{fin}} \ll E_{\text{init}}$ and almost all initial kinetic energy of the system is radiated away.

The situation is a bit more complicated when the second blob, which represents the CSM envelope, is not static at the time of the explosion, but expands with a momentum \mathbf{p}_2 . This is most probable for the case of SLSNe I, because velocities higher than 10,000 km/s are observed for several months starting from the maximum (Liu et al 2017b). The energy before the interaction in this case is the sum of ejecta and CSM energies. In the prescription of two blobs, that is the sum of the blobs' energies:

$$E_{\text{init}} = \frac{\mathbf{p}_1^2}{2m_1} + \frac{\mathbf{p}_2^2}{2m_2}. \quad (4)$$

After the inelastic interaction the kinetic energy of the system becomes

$$E_{\text{fin}} = \frac{(\mathbf{p}_1 + \mathbf{p}_2)^2}{2(m_1 + m_2)}. \quad (5)$$

So an amount of energy that can be thermalized during the interaction is

$$\Delta E = E_{\text{init}} - E_{\text{fin}} = \frac{(\mathbf{p}_1 m_2 - \mathbf{p}_2 m_1)^2}{2m_1 m_2 (m_1 + m_2)} = \frac{m_1 m_2}{2(m_1 + m_2)} (\mathbf{v}_1 - \mathbf{v}_2)^2. \quad (6)$$

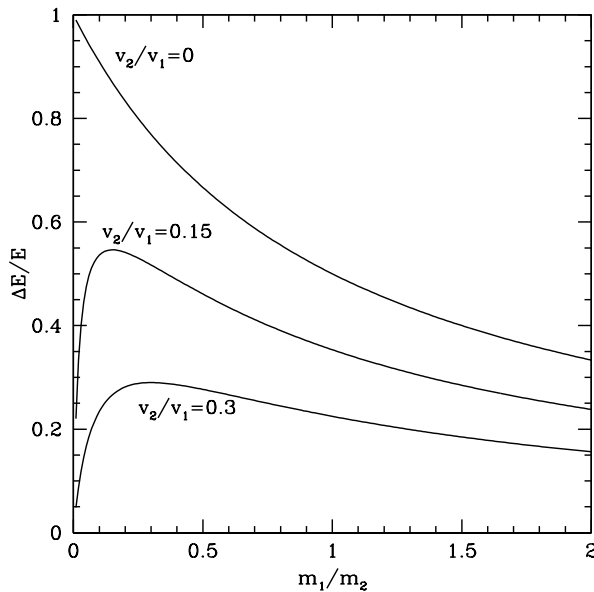


Fig. 3 Energy losses relative to the initial kinetic energy of the system of two inelastically colliding blobs.

Here \mathbf{v}_1 and \mathbf{v}_2 are velocities of the colliding blobs that represent, respectively, the ejecta and the CSM envelope. Again, the important question is how much of the total kinetic energy of the system can be lost to radiation, because for the superluminous event this energy transformation must be very effective. If we define $\mu = m_1/m_2$ and $\beta = v_2/v_1$ then we get

$$\frac{\Delta E}{E_{\text{init}}} = \frac{\mu(1 - \beta)^2}{(\mu + 1)(\mu + \beta^2)}. \quad (7)$$

It is clear that $v_1 > v_2$ ($\beta < 1$). Otherwise, the collision will never happen. This means that the larger the difference between v_1 and v_2 , the larger the energy that can be radiated. For a few fixed values of β , the dependence of $\Delta E/E_{\text{init}}$ on the mass ratio μ is shown in Fig. 3. When the CS envelope is expanding ($v_2 > 0$) the maximum losses happen not at $m_1 \sim 0$, but at some finite mass. Still, m_1 has to be noticeably lower than m_2 for the effective energy loss to happen. This means that the ejecta must be less massive than the CS envelope for a SLSN event.

Typical radius. A crude estimate yields the photospheric radius R_{ph} , and, therefore, the typical size of the dense circumstellar envelope that can provide the observed luminosity L of the SLSNe. For simplicity, assume that the SLSN emits like a blackbody with a temperature T_{bb} . Then the photospheric radius can be obtained from $L = 4\pi R_{\text{ph}}^2 \sigma T_{\text{bb}}^4$. The typical temperature measured for SLSNe is $T_{\text{bb}} \simeq 10^4$ K. The order of magnitude estimate of the luminosity is $L \simeq 10^{44}$ erg/s. Hence, the radius is roughly

$R_{\text{ph}} = 4 \times 10^{15}$ cm, which is about an order of magnitude larger than typical photospheric radii of standard SNe near maximum light.

Ginzburg and Balberg (2012) in their simple numerical hydrodynamic diffusion model got a similar value for the CSM radius (of order 10^{15} cm), and also stated that the masses of the ejecta and the CSM involved into the interaction must be comparable for the effective transformation of energy into radiation. As we see from the Fig. 3, a smaller ejecta-to-CSM mass ratio is even better.

4.2 Hydrodynamical properties

Shock propagation through the optically thick extended CSM. The shock waves produced at the ejecta-CSM interaction are initially radiation-dominated. The photons behind the shock bear a large amount of energy compared to the gas energy. The photons are locked within the CSM and heat it up making the shock front wider. Precursor heating extends to the optical depth $\tau = c/v_s$ from the shock front, where v_s is a shock velocity. When it reaches the outer edge of the CSM, the photons that were heated on the shock start to gradually leave the system. The shock begins to break out. Due to the large size of the system the breakout stage lasts much longer than it does for standard SN Ib/c. In the latter case, $R < 10 R_{\odot}$ and the shock breaks out for less than $R/v_s \sim 200$ s, while in the case of CSM-interacting SLSN with typical $R \sim 10^5 R_{\odot}$, the shock breakout time is proportionally larger and lasts a few months. On the whole the light curve of the SLSNe in the CSM-interaction scenario can be considered as a prolonged shock breakout. At some stage the shock can become strongly radiative. The temperature jump at the shock almost disappears, and the shock becomes almost isothermal. In this case, the density can jump up by a few orders of magnitude, and a rather dense and thin layer forms behind the shock. A very detailed study of the structure of the SN shocks is provided by Weaver (1976). More details are presented in Tolstov et al (2015). The basic formulas can be found in Blinnikov (2016).

Fig. 4 shows the results of a numerical calculation of the ejecta-CSM interaction for one of the SLSN models that demonstrates how the radiative shock propagates throughout the dense extended CSM and what happens with the Rosseland optical depth (and therefore, photospheric radius) at the same time. While the CS envelope is cool before the SN explosion, it is transparent to the radiation, but when it becomes warm due to the pre-heating by the photons from the shock, it quickly becomes optically thick and strongly diffusive. The photosphere ($\tau_{\text{R}} \sim 1$) shifts to the outer edge of the CSM. As a result, the shock is left deep inside the photosphere for a few months. Conditions are not appropriate for hard emission at the early stages despite the high velocity of the shock. But an ultraviolet flash, or perhaps even an X-ray flash, can appear later, when the shock becomes weaker, closer to the outer edge of the CS envelope. This can happen in the fading stage of the light curve evolution. SCP 06F6 is a possible example of such a SLSN originating from interaction due to the X-ray flash observed about 2 months after the maximum (Gänsicke et al 2009). At the earlier stage, near

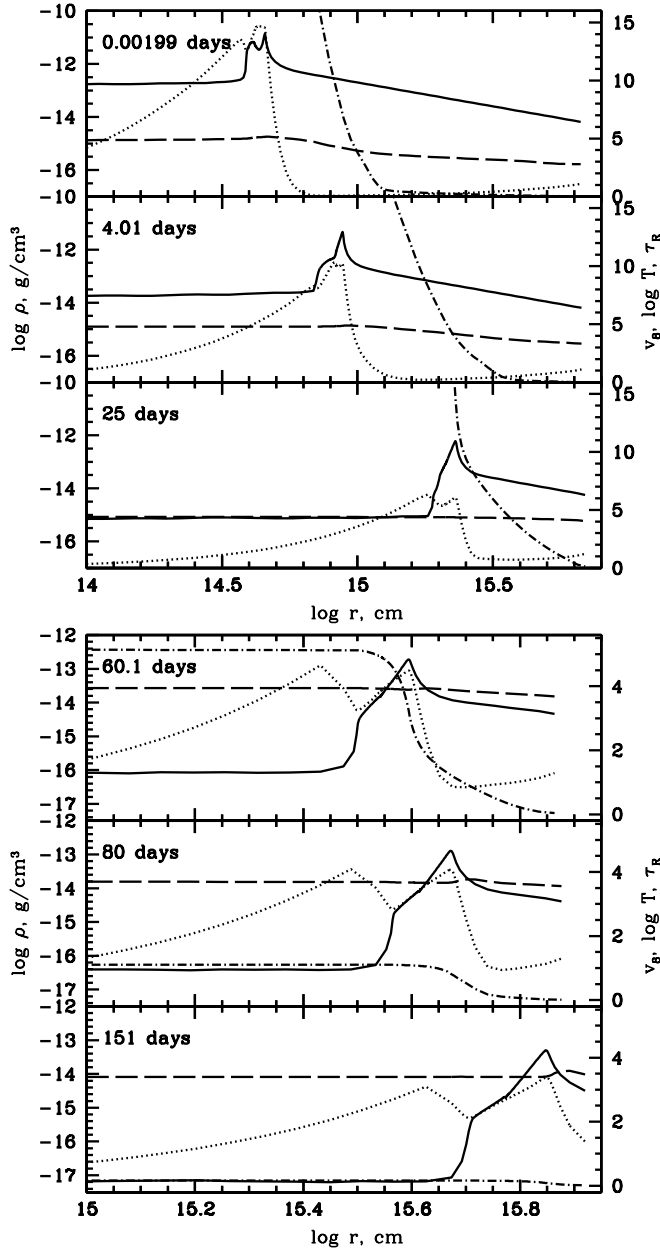


Fig. 4 Evolution of radial profiles of the density (*solid lines*), velocity (in 10^8 cm s^{-1} , *dots*), gas temperature (*dashes*), and Rosseland optical depth (*dash-dots*) for the model N0 from Sorokina et al (2016). The scale for the density is on the left Y axis, for all other quantities, on the right Y axis. Upper panel: pre-maximum hydrodynamical structure for three moments, very soon after the explosion and at days 4 and 25. Lower panel: the same parameters, but after maximum, at days 60, 80, and 151. Note that different scales for the axes are used on the upper and lower panels.

maximum, the temperature conditions are appropriate for strong emission in the near UV range. Almost all SLSNe are relatively blue near maximum, and the shock heating in the CSM interaction scenario reproduces the color better than other mechanisms (Tolstov et al 2017b).

4.3 Light curves

Analytical models. Analytical methods to obtain rough estimates for the interaction-powered SNe are available. In this review, we focus more on numerical studies and we only briefly mention the analytic studies.

The dense CSM required to explain the large luminosity of SLSNe by the interaction is optically thick and we need to take large optical depths of the dense CSM into account in treating them analytically unlike the case of less luminous Type II SNe (e.g., Chevalier and Fransson 2003, Moriya et al 2013b). When the CSM optical depth is large enough, the shock breakout itself can occur in the dense CSM. Chevalier and Irwin (2011) provide a simple analytic way to estimate the rise time and peak luminosities followed by the shock breakout in the dense CSM. They show that the LC features differ depending on where the shock breakout occurs in the dense CSM. This method is extended to the case of non-steady mass loss by Moriya and Tominaga (2012).

Chatzopoulos et al (2012, 2013) develop a semi-analytic approach to estimate the overall LC properties of the interaction-powered SNe that are commonly used recently. Although it is a simple powerful method to estimate the CSM properties, it is important to keep its limitation in mind. The semi-analytic method is based on the formalism of Arnett (1980) that assumes that the heating source is at the center of SNe. However, the energy source of the interaction model is not located at the center. It moves outwards as the shock progresses. Moreover, it can be situated within a very thin layer, since gas between the forward and the reverse shocks can cool down strongly. In this case, it is almost impossible to spatially separate the emission from the two shocks, while the analytic solution by Chatzopoulos et al (2012, 2013) takes the radiation of the forward and the reverse shocks into account separately, which leads to an inaccurate luminosity prediction. Indeed, the CSM configuration obtained by the semi-analytic model has been shown to be inconsistent with those found by numerical approaches (Moriya et al 2013a, Sorokina et al 2016). Chatzopoulos et al (2013) study how to find the CSM configuration from the semi-analytic model that better matches the numerical results.

Numerical modeling. Numerical modeling allows taking more physical processes into account and simulating them in detail, so the results should be more robust.

The interaction scenario is challenging for numerical modeling. A numerical code must be able to resolve optically thick shocks. This is a reason why the number of SLSN interaction models calculated up to now is not very large. The very first numerical modeling of the SN ejecta interaction with the dense extended medium has been done by Grasberg et al

(1971), Falk and Arnett (1977), Grasberg and Nadyozhin (1987). More recently, most calculations were produced with the radiation hydrodynamic code STELLA (Blinnikov et al 1998, 2006).

SLSNe II. Hydrogen-rich SLSNe are spectroscopically similar to SNe IIn, and therefore, their origin from the interaction of SN ejecta with slowly expanding dense CSM is the most probable scenario. To provide the high luminosity of SLSN, the CSM is expected to be sufficiently more massive than for SN II case.

Woosley et al (2007) suggest a pulsational pair instability (PPI) scenario for the last stage of the pre-SN evolution, which leads to the formation of the required density structure. PPI can happen for stars with an initial main-sequence mass 95–130 M_{\odot} , or, more certain, with a helium-core mass 40–60 M_{\odot} . Near the end of their lives, when the central temperature exceeds 10^9 K, such stars lose stability through electron-positron pair creation. Explosive oxygen burning in the cores of these stars cannot unbind the whole star, but leads to the ejection of a very massive envelope with large kinetic energy. The remaining stellar core contracts, and some time later, when the central temperature again becomes high enough for pair creation, another ejection happens. The process repeats until the stellar mass becomes too low for the pair instability, and the core finally collapses due to iron dissociation.

As a result of the PPI scenario, the final core collapse happens inside the system of the massive expanding shells. Collision of these shells, as well as of the final ejecta with shells, can lead to a very bright event, as observed for the SLSNe.

Woosley (2017) presents a wider study of the models of the stellar evolution exploding as PPISNe. He concludes that no solar metallicity star ends up as PPISN since it loses too much mass through the wind, while stars with the metallicity $Z/Z_{\odot} < 0.1$ can lead to this end. For SLSNe II, whose host galaxies have metallicities in a wide range, including high-metallicity objects (Perley et al 2016), this means that the PPI explosion mechanism is not so likely to explain all these events, though more study of PPI is still required. At the same time, PPI may be promising to explain SLSNe I, since they prefer low-metallicity galaxies and their photospheric velocities are much larger than what more standard stellar mass loss mechanism can provide.

Woosley et al (2007) apply the PPI scenario to one of the first SLSN II, namely, SN 2006gy. They found that the collisions of two subsequent mass ejections of about 25 M_{\odot} and 5 M_{\odot} , separated in time by less than 7 years, with a total energy of about 3×10^{51} ergs, provides a good fit to the observed light curve of SN 2006gy.

Moriya et al (2013a) studied a large number of toy models for the colliding ejections and found slightly different parameters for the best-fit model for SN 2006gy. Both ejections contain a mass of about 15 M_{\odot} (the second one could be lighter), and their kinetic energy is 4×10^{51} ergs, which is only a little larger than the energy of normal SNe. The influence of the density distribution on the light curve is also studied, which showed that the first ejection could not be formed by a steady wind.

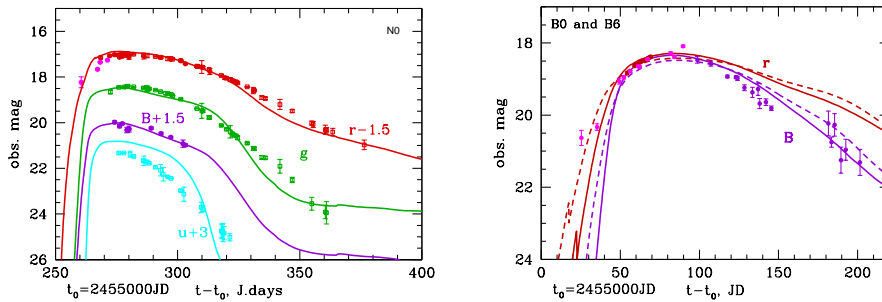


Fig. 5 The narrow light curve of SN 2010gx (*left*, Pastorello et al 2010) and the broad one of PTF09cnd (*right*, Quimby et al 2011) in different filters. Observations are shown with *dots*, calculations (Sorokina et al 2016) with *lines*. *Solid* and *dashed* lines in the right plot mean different composition: *solid* lines correspond to the model B0 with the outer envelope containing 90% carbon and 10% oxygen, *dashed* lines correspond to the model B6 similar to B0, but roughly half of C and O in the outer envelope is replaced with He.

Despite a slightly different estimate of the ejection parameters, both Woosley et al (2007) and Moriya et al (2013a) converge on the conclusion that two subsequent ejections of a mass of a few tens solar mass with an energy close to the typical one for SN explosions within a few years can easily lead to the very high luminosities typical for SLSNe. Similar results are obtained by Dessart et al (2015) and Vlasis et al (2016), who also investigate aspherical CSM configurations.

SLSNe I. In the modeling of hydrogen-poor SLSNe, one more parameter appears in addition to those that are important for hydrogen-rich events. It is the chemical composition of the ejecta and the CSM. There are several observational hints for choosing the correct composition for numerical modeling of SLSN I light curves and spectra. Observationally, strong broad oxygen lines are typical for SLSNe I from the very beginning, but very few SLSNe I have helium lines in their nebular spectra. So the observations favor a CO composition for the ejecta and CSM. Numerical modeling of the multicolor broad-band light curves (Sorokina et al 2016) is in agreement with the observations from this point of view. The presence of helium leads the light curve to rise much longer than observed, while a CO composition results in a faster rise. This difference is explained by different opacities for CO and He. CO material requires a lower temperature for excitation and ionization, so the carbon-oxygen CSM becomes opaque soon after the shock starts to heat the CSM gas in front of it. Helium needs a higher temperature to become opaque, and it takes a longer time. Some amount of helium can be mixed with the CO gas. The light curve is not much changed when carbon and oxygen are the main absorbers. The photometric colors near maximum help determine the proportions of C to O, since these elements have different spectral line distributions. Oxygen is more absorptive in the blue, and it shifts the larger part of the emission to this wavelength range. The modeling by Sorokina et al (2016) shows that models with a C to O ratio from 0.7 to 0.9 show the best fit to the observations of the narrow and the broad SLSN I light curves, respectively. The light curves

are shown in Fig. 5, and demonstrate how the pure ejecta–CSM interaction scenario, without any radioactive material, can reproduce the emission of SLSNe I. The masses and energies of the models are similar to those needed for SLSNe II. A fast evolving SLSN I can be reproduced by the interaction with about $10 M_{\odot}$ CS envelope, while for slowly fading events, a few tens M_{\odot} of hydrogen-poor material is needed. The explosion energy in any case is a few 10^{51} erg.

Bumpy light curves. Light curves of some SLSNe I show some undulations on the fading part (Inserra et al 2017). The CSM interaction scenario explains this in the most natural way: each bump on the light curve can denote the collision of CSM layers or the SN ejecta with a CSM layer. If the progenitor star experiences several episodes of massive ejection before the final collapse as it can happen in the PPI mechanism, then several collisions of CSM layers could be later observed as bumps on the SLSN light curve. In the spectra of the SLSNe I with the most undulating light curves, hydrogen lines appear at a late stage (Yan et al 2017a). This also can be considered as a proof for the CSM interaction scenario for some SLSNe I. Initially the luminosity of the SLSN is explained by the collision of the innermost hydrogen-free layers, while the outer layers that can contain some hydrogen are cold and transparent. Later, the inner hydrogen-poor layers, that are faster, reach the hydrogen-rich one, heat it, and the hydrogen lines appear in the spectrum.

The origin of the early pre-maximum luminosity excess that is observed in many SLSNe I is more questionable. Moriya and Maeda (2012) qualitatively explain the possible origin of this excess by heating of a detached CS envelope. Its opacity is enhanced after ionization leading to a temporary decrease in luminosity before a rise to the main maximum. More detailed numerical modeling is needed for this mechanism. Some other explanations of the pre-maximum excess are described in Sect. 6.

4.4 Pros and cons for the interaction scenario

Summarizing the above material, we point out the strengths and weaknesses of the CSM interaction model for SLSNe.

The interaction scenario for SLSNe is favored due to the following reasons:

- SLSNe II are spectrally very similar to SNe IIn that are explained by CSM-ejecta interaction. For a more massive CSM, a more luminous (and superluminous) SN is expected.
- SLSN I light curves with a wide range of rising and fading timescales can quite easily be modeled by the interaction with a CSM of different mass. The larger the light curve timescale, the more massive CSM is needed. Only the widest light curves are problematic for modeling with interaction.
- The undulation on the fading part of the light curve is most naturally explained by a sequence of collisions of several CSM envelopes or clouds.

-
- Measuring masses of different elements from the nebular spectra of SLSNe (Jerkstrand et al 2017), energetics of these events, and other observational properties show that SLSNe originate from massive stars. Mass loss is typical for these objects (Vink 2015). In this sense, some kind of CSM interaction is unavoidable after the SN explosion. However, the amount of such material must be very large to provide the strong interaction that is required to explain the SLSN phenomenon.

The last item from the list above takes us to the list of difficulties that still remain for the interaction mechanism.

- At least a few solar masses must be lost by a SLSN progenitor during a few months before the explosion to explain the brightness and the duration of the SLSN events. Although this is not impossible from the stellar evolution point of view, there is no detailed understanding of the very last stages of stellar life yet, neither theoretical, nor observational. The required CSM mass is comparable to observed mass-loss rates only from luminous blue variables (LBVs) in outburst (Smith et al 2011). For the metal-poor stars that are able to preserve considerable mass without losing it through a steady wind till the end of their evolution, eruptive mass loss with the ejection of several solar masses of gas prior to the explosion could be very important (Smith and Owocki 2006). Anyway, a detailed mechanism for the LBV eruptions is still unknown, as well as the details of the mass loss by the PPI mechanism. It is not, of course, an argument against the origin of SLSNe from CSM interaction, but this topic still requires both theoretical and observational efforts.
- High photospheric velocities (10,000 – 20,000 km/s) are measured in SLSNe I for about a month from maximum. Existing numerical interaction models do not reproduce these velocities. But an explosion energy only a little larger than standard has been considered in modeling. Enhancing the explosion energy up to a few 10^{52} erg and the kinetic energy of the CSM expansion to about 10^{51} erg can improve the situation. However, this energetic model would bring another problem: such energetic explosions must be separated in time longer than needed for getting a strong interaction because the stronger an eruptive mass ejection is, the longer time is needed for the star to reach the instability conditions for the next explosion or eruption. For example, an estimate of the time intervals between the eruptions for the PPI model can be found in Woosley (2017).
- The slowest (i.e., widest) observed SLSN I light curves together with high velocities are extremely difficult to explain solely by CSM interaction. In this case a combination of energy sources, like CSM interaction for the maximum plus radioactivity for the tail similar to what has been done in Tolstov et al (2017a,b), is more promising.

Detailed numerical modeling for an extended set of explosion parameters is still needed to understand the applicability of the CSM interaction model to the SLSNe, especially for the hydrogen-poor ones. Not only the light curves must be fitted, but also the spectra. PPI seems to be the best mechanism for making a CSM density and velocity structure that would

lead to a SLSN event after the interaction with the SN ejecta. But PPI itself must be better studied in order to understand the limitations it places on the CSM structure.

5 Magnetar-powered models

The view that pulsars could play a role in powering supernovae was proposed soon after the discovery of pulsars. Ostriker and Gunn (1971) proposed that the spin-down of a central pulsar could power both the supernova explosion and the light from the supernova. In this model, the pulsar creates a bubble of relativistic fluid that sweeps up and then accelerates the surrounding star. However, this model was not found to be in accord with supernova observations. The current prevailing model is that the power for the supernova is injected over a short period of time (seconds) and the pulsar bubble then evolves in the freely expanding ejecta set up by the initial explosion. This model was proposed for the Crab Nebula and other young pulsar wind nebulae (Chevalier 1977) and for the light from supernovae (Gaffet 1977). Generally, the light from core collapse supernovae does not require power input from a pulsar, and can be explained by a combination of initial explosion energy, radioactivity, and possible circumstellar interaction. However, the supernova SN 2005bf showed two broad peaks, implying the operation of some additional mechanism in addition to the usual. Maeda et al (2007) suggested that power from pulsar spin-down could be the source of the additional power. The observed luminosity and timescale required a highly magnetized pulsar ($> 10^{14}$ G), or magnetar, with an initial spin period in the ms range. Kasen and Bildsten (2010) and Woosley (2010) found that similar parameters could explain the timescale and luminosity of SLSNe, and this has become one of the leading contenders for the light from SLSNe. Here we discuss the basic magnetar model, giving some of the uncertainties of the model. We primarily deal with simplified models that illustrate the physical principles.

The initial central explosion is assumed to occur on a timescale of seconds, followed by shock traversal of the star and the ejecta transition to free expansion on a timescale of the doubling of the radius. At that point, the velocity profile is given by $v = r/t$. The density profile for the expanding gas can be approximated as a steep power law with radius at large radii and a flat power law at small radii (Chevalier and Soker 1989, Matzner and McKee 1999). We have the inner power law $\rho_{in} \propto t^{-3}(r/t)^{-\delta}$ and outer $\rho_{out} \propto t^{-3}(r/t)^{-n}$. Here, we take $\delta = 0$. The transition velocity between the inner and outer density profiles is

$$v_{tr} = \left[\frac{10(n-5)}{3(n-3)} \frac{E_s}{M_{ej}} \right]^{1/2}. \quad (8)$$

For $n = 7$, we have $v_{tr} = 4080 E_{51}^{1/2} M_5^{-1/2}$ km s $^{-1}$, where E_{51} is E_s in units of 10^{51} ergs and M_5 is M_{ej} in units of $5 M_\odot$, where E_s is the supernova energy and M_{ej} is the ejecta mass. The value of E_s is generally taken to be

1×10^{51} ergs, which is a value that is obtained for cases where the energy is well determined.

The newly formed rapidly rotating neutron star is assumed to drive a supersonic/superAlfvénic wind, powered by the spin-down of the neutron star. The details of how the transition is made from an accreting neutron star to a pulsar wind are not known. A plausible estimate for the spin-down power is the result for a force-free magnetic field (Spitkovsky 2006)

$$\dot{E} \approx \frac{\mu^2 \Omega^4}{c^3} (1 + \sin^2 \alpha), \quad (9)$$

where $\mu = BR^3$ is the magnetic dipole moment, $\Omega = 2\pi/P$ is the spin frequency, α is the angle between the magnetic and rotation axes, B is the dipole field at the neutron star surface, and R is the neutron star radius. Here, R is taken to be 10 km. The neutron star rotational energy is $E = \frac{1}{2}I\Omega^2$ where I is the neutron star moment of inertia, taken to be 1×10^{45} gm cm². The initial spin-down time is

$$t_{sd} = \frac{E_0}{\dot{E}_0} = 0.14 \left(\frac{P_0}{\text{ms}} \right)^2 \left(\frac{B_p}{10^{14}\text{G}} \right)^{-2} \text{ day}, \quad (10)$$

where the subscript 0 refers to the time $t = 0$. The evolution of the spin-down power is given by

$$\dot{E} = \dot{E}_0 \left(1 + \frac{t}{t_{sd}} \right)^{-2}. \quad (11)$$

The structure of pulsar magnetospheres is not a fully solved problem; there are other possibilities for the spin-down. For the vacuum magnetic dipole case

$$\dot{E}_{vac} = \frac{2\mu^2 \Omega^4}{3c^3} \sin^2 \alpha. \quad (12)$$

In the force free case, there is spin-down for an aligned rotator, but not in the vacuum case.

More generally, the evolution of the spin of a pulsar is often taken to be of the form

$$\dot{\Omega} \propto -\Omega^m \quad (13)$$

where m is the braking index. The value of m for the magnetic dipole case is 3 and the constant of proportionality in that case can be related to the neutron star moment of inertia and magnetic field, as discussed above. The value of m can be determined from observations by $m = \ddot{\Omega}\Omega/\dot{\Omega}^2$. The power from the spin-down with constant m is

$$\dot{E} = \dot{E}_0 \left(1 + \frac{t}{\tau} \right)^{-(m+1)/(m-1)}, \quad (14)$$

where τ is a spindown timescale that cannot now be written simply in terms of the magnetic field. Measured values of m for ordinary pulsars are < 3 . For PSR J1119–6127, $m = 2.91$, close to the magnetic dipole value. Other

values are lower; the long term value is $m = 2.34$ for the Crab Pulsar and 1.7 for the Vela pulsar (Espinoza et al 2017). Possible reasons for deviations from the magnetic dipole value are evolution of the neutron star moment of inertia or magnetic field, or a more complex magnetic configuration than a dipole. These considerations show that pulsars generally do not follow the magnetic dipole spin-down and the late evolution of \dot{E} (at $t \gg \tau$) is steeper than in the force-free dipole case; for the case of the Vela pulsar, $\dot{E} \propto t^{-3.9}$ at late times. The parameters for the rapidly rotating magnetars of interest here are quite different from the ordinary pulsars, but these objects show that pulsar spin-down can deviate from the force-free dipole case.

We next consider the evolution of the pulsar bubble on the assumption of adiabatic motion. In the case of a pulsar wind nebula, the shocked pulsar wind of relativistic particles and magnetic field can be approximated by a $\gamma = 4/3$ fluid, where γ is the adiabatic index. For the relatively young SLSN case, the assumption is that the pulsar power thermalizes so the radiation field is the dominant energy density. Again, an initial value $\gamma = 4/3$ is appropriate. If spherical symmetry is assumed, the expansion of the pulsar bubble can be found in the thin shell approximation. Even if the outer shock wave is not radiative, the swept up shell is thin. If the pulsar provides a steady power \dot{E} , the radius of the swept up shell is (Chevalier 1977, Blondin et al 2001)

$$R_s = 1.50 \left(\frac{n}{n-5} \right)^{1/5} \left(\frac{n-5}{n-3} \right)^{1/2} \left(\frac{E_s^3 \dot{E}^2}{M_{ej}^5} \right)^{1/10} t^{6/5}, \quad (15)$$

where the thin shell approximation has been made. We have

$$t_{tr} = \frac{66(n-5)}{25n} \frac{E_s}{\dot{E}}, \quad (16)$$

where t_{tr} is the time for the shell to reach the inflection point in the supernova density profile. Approximating $\dot{E} = E/t_{sd}$ for a time t_{sd} , we have

$$t_{tr} = 0.19 B_{14}^{-2} P_{ms}^4 E_{51} \text{ day}. \quad (17)$$

Once the shell has traveled through the flat part of the supernova density profile, it comes into the steep power law part of the density profile. The mass added from the outer ejecta is negligible compared to that in the shell and, for 1-dimensional (1-D) expansion, the evolution of the shell radius goes to $\propto t^{1.5}$ as in the solution of Ostriker and Gunn (1971). This is another self-similar solution.

The acceleration of the shell by the hot bubble is subject to Rayleigh-Taylor instability (RTI). The action of the RTI while the shell is in the flat part of the ejecta density profile has been well studied (Porth et al 2014, Bucciantini et al 2004). Despite the growth of instabilities, the instability saturates and the flow remains self-similar; the outer shock front has a radius that is 7% larger than in the 1-D solution (Blondin and Chevalier 2017). Most of the swept up mass is in the shell, although there is also some matter that is in fingers that extend in towards the neutron star. The RT

fingers have relatively little effect on the termination shock of the pulsar wind. Global simulations including a magnetic field show qualitatively similar properties, although the Kelvin-Helmholtz instability is suppressed on small scales.

Once the shell reaches the transition point in the density profile, there is a qualitative change in the evolution. The preshock ejecta are unable to contain the pressure of the shocked wind bubble (Chevalier 2005) and the bubble matter blows out through the shell (Chen et al 2016, Suzuki and Maeda 2017, Blondin and Chevalier 2017). Channels form in the swept up ejecta through which matter from the inner wind bubble flows. Suzuki and Maeda (2017) used a special relativistic code, allowing for a relativistic pulsar wind that shocked and slowed on passing through the termination shock. When the gas was able to escape through channels, relativistic velocities were again attained.

The power provided by the magnetar initially comes out in a relativistic wind of particles and Poynting flux. Assumptions must be made about the fraction of the wind power that goes into thermal radiation field. There might also be some fraction that remains in nonthermal form. The mechanisms giving rise to thermalization are not well understood.

Standard models for calculating the light curves of SLSNe I (Chatzopoulos et al 2012, Inserra et al 2013, Nicholl et al 2017b) have been proposed based on the formalism developed by Arnett (1980, 1982) for ordinary supernovae. The model assumes that the supernova gas is homologously expanding and is characterized by a constant opacity κ for the thermal radiation. The emitted luminosity is

$$L(t) = 2e^{-(t/t_d)^2} \int_0^t e^{(t'/t_d)^2} \frac{t'}{t_d} \dot{E}(t') \frac{dt'}{t_d}. \quad (18)$$

where

$$t_d = \left(\frac{10\kappa M_{ej}}{3\beta v_{ej} c} \right)^{1/2} \quad (19)$$

is a diffusion time that gives a characteristic timescale for the light curve, v_{ej} is the velocity at the outer edge of the ejecta, and c is the speed of light. Here, β is a constant that depends on the density distribution of the freely expanding ejecta. We have $\rho_{ej} \propto \exp(1.723Ax)$, where A is a constant and $x = r/v_{ej}t$. For uniform density ejecta ($A = 0$), $\beta = 13.8$ and for $A = -1$, $\beta = 13.4$; $\beta = 13.8$ is typically chosen in magnetar models. As discussed above, a fairly flat density distribution is a reasonable approximation for the freely expanding ejecta in a core collapse supernova. However, in the present case, the density distribution is strongly affected by the magnetar wind nebula, causing some uncertainty in the model fits.

There is the assumption in equation (18) that the initial stellar radius is much smaller than the supernova radius so that terms involving the initial radius and thermal energy do not appear. The initial explosion energy is lost to adiabatic expansion. Another assumption in equation (18) is that all the pulsar power goes into the thermal radiation, but it may only be some fraction f that is thermalized. There have been various suggestions

on how nonthermal effects can be included. Kotera et al (2013) suggested that a constant fraction of the pulsar power goes into the thermal radiation. However, Wang et al (2015) noted that models using equation (18) fit the observations at early times, but fall below the observations at late times. They suggested that

$$f = 1 - e^{Bt^{-2}}, \quad (20)$$

where

$$B = \frac{3\kappa_\gamma M_{ej}}{4\pi v_{ej}^2} \quad (21)$$

and κ_γ is the opacity for high energy photons. This expression has the property that at early times, nonthermal photons are completely thermalized, and at late times there is optically thin absorption of photons, assuming that the absorbing material is uniform.

This model, or some variation on it, has been widely used in modeling the light curves of SLSNe I. Different researchers make different assumption, hindering the comparison of results. Nicholl et al (2017b) have analyzed the light curves of 38 SLSNe I in a consistent way, using the radiative transfer approximation of Arnett and the energetic photon escape of Wang et al (2015). They assumed the vacuum magnetic dipole spindown for the pulsar power and made a blackbody assumption to obtain multi-color light curves for the supernovae. A result of their model fitting is shown in Fig. 6. The models fit the cases with a decline that mimics that of ^{56}Co , like SN 2007bi. They deduce the following ranges (1-sigma) of parameters from their models: initial period 1.2–4 ms, $B = (0.2 - 1.8) \times 10^{14}$ G, and $M_{ej} = (2.2 - 12.9) M_\odot$. Using similar methods, Liu et al (2017a) had previously modeled 19 supernovae and obtained good fits for 14 objects. They found parameter ranges: initial period 1.2–8.3 ms, $B = (0.2 - 8.8) \times 10^{14}$ G, and $M_{ej} = 1 - 27.6 M_\odot$. These results give some idea of the range of parameters in present modeling. Yu et al (2017) also modeled 31 SLSNe similarly and found parameter ranges of initial period 1.4–12 ms, $B = (0.5 - 4.8) \times 10^{14}$ G, and $M_{ej} = 0.5 - 17.9 M_\odot$.

Most modeling efforts have concentrated on the supernova light curves, but there has also been attention to the spectra of SLSNe. Dessart et al (2012) calculated steady-state, 1-D, non-LTE spectral models with power input from a magnetar. They found that the magnetar has important effects when the energy deposited by the magnetar becomes comparable to the supernova energy. In this case, the spectrum is blue, in accord with observations, and does not have the line-blanketing that occurs when the power is produced by radioactivity. Broad lines can be produced, as observed, if the ejecta mass is relatively small.

Bersten et al (2016) also went beyond the simple models in their light curve models, using a 1-D, special relativistic, radiation hydrodynamics code. They found that hydrodynamical modeling is especially important when the deposited magnetar energy exceeds that of the initial supernova, consistent with the arguments given above.

Although the magnetar model has had considerable success in reproducing the light curves and spectra of SLSNe I, these results follow from a

certain power supplied over a certain time and do not provide a “smoking gun” for the magnetar model. There has been interest in whether some of the detailed features of SLSN I observations require a magnetar. As noted in Section 2.2, some SLSNe I show a precursor in the light curve before the main peak. Kasen et al (2016) suggested that the precursor is emission from the breakout of the shock wave driven by the pulsar wind bubble. However, the power generated by the shell sweeping into the freely expanding ejecta is small. In order to obtain a significant precursor, Kasen et al (2016) suggest that only a fraction of the initial pulsar power is thermalized, reducing the main peak relative to the shock breakout. Other suggestions for the precursor emission include circumstellar interaction (Moriya and Maeda 2012, Piro 2015) or a highly energetic supernova (Nicholl et al 2015b).

Metzger et al (2014) have discussed the breakout of an ionization front through the swept up shell. They assume that a substantial fraction of the pulsar power goes into an ionizing spectrum radiated by energetic particles. The ionization front is initially trapped in the shell but it is able to penetrate the shell as the column density of the shell declines due to expansion. This breakout can occur within months of optical maximum under certain conditions. Accounting for the Rayleigh-Taylor instability of the shell would result in an earlier breakout if the pulsar wind evolves to this phase. The ionization breakout theory was proposed in part to explain the luminous X-ray emission observed from SCP 06F6 (Levan et al 2013). The complete ionization of the shell allows the X-rays to escape. However, after the detection with XMM, an observation with Chandra set a low upper limit on X-rays from SCP 06F6, and X-ray observations of other SLSN have only yielded upper limits (Margutti et al 2017).

There may be a connection between SLSNe and long gamma-ray bursts (LGRBs). Both classes of objects occur in small, low metallicity galaxies. An ultra-long GRB, GRB 111209A, has recently been observed along with a bright supernova, SN 2011kl (Greiner et al 2015). Margalit et al (2018) suggest that the two classes of objects have similar progenitors (rapidly rotating neutron stars) and that the alignment between the spin axis and the magnetic axis is what determines the relative amount of jet vs thermal emission. In this view, the aligned rotator case is expected to give strong jets. The importance of jets in SLSNe is also discussed in, e.g., Soker and Gilkis (2017), Gilkis et al (2016).

Although the magnetar model has attractive features, the case is not yet settled. The multidimensional hydrodynamic models show that a complex 3-D structure results from power input from an energetic magnetar (Chen et al 2016, Suzuki and Maeda 2017, Blondin and Chevalier 2017). Models that account for that structure are ultimately needed.

We summarize pros and cons of the magnetar-powered models.

Pros:

- The magnetar models can explain both the slowly declining and the rapidly declining light curves of SLSNe Ic.
- The observed velocities and temperatures are roughly reproduced.

Cons:

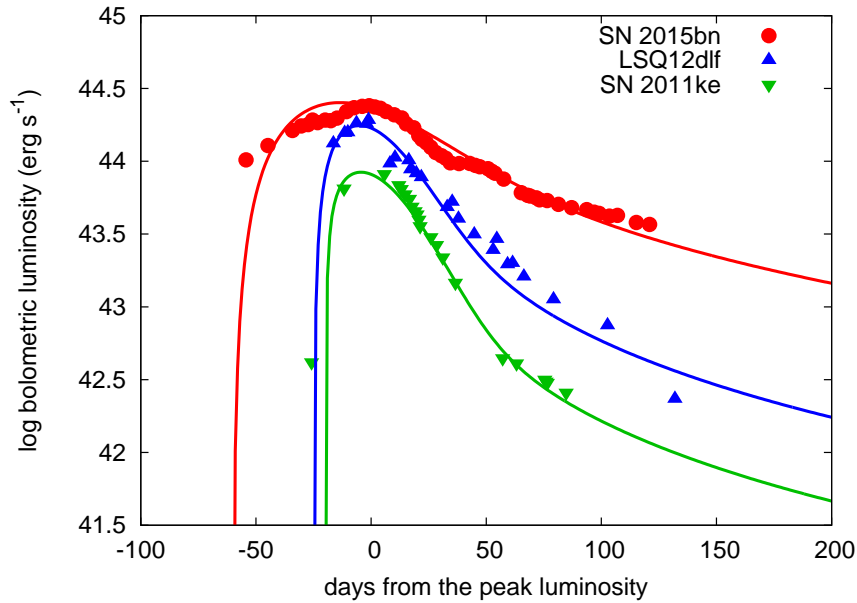


Fig. 6 Examples of magnetar-powered LCs fitted to SLSNe with different LC evolution. The SLSN bolometric LCs are obtained from Nicholl et al (2016b). The model LCs are calculated with a semi-analytic way based on Arnett (1982) as in Inserra et al (2013). The magnetar spin down energy is assumed to be thermalized with 100% efficiency. The magnetic field strengths and the spin periods in the models are: 10^{14} G and 2 ms (SN 2015bn), 3.5×10^{14} G and 2.5 ms (LSQ12dlf), and 7×10^{14} G and 2.5 ms (SN 2011ke).

- The magnetar models have a number of free parameters. There is not a “smoking gun” for the presence of magnetar power.
- The magnetar models do not naturally explain the bumps observed in the light curves of some SLSNe.

6 Comparison

Here we compare the three major suggested mechanisms discussed so far. SLSNe II_n show clear signatures of CSM interaction and their LCs and spectra can be explained by the interaction-powered model (Section 4). We here focus on SLSNe Ic whose luminosity sources are actively discussed now.

6.1 Light curves

Both interaction-powered and magnetar-powered models can provide reasonable fits to most SLSN Ic LCs with a proper choice of the model parameters. The ^{56}Ni powered models fail to explain the rapidly declining

SLSN Ic LCs as their late-phase luminosity evolution is governed by the nuclear decay rate of ^{56}Co which is rather slow.

Some SLSN Ic LCs show complicated structures that may prefer the interaction model. For example, the LCs of iPTF15esb (Yan et al 2017a) have two major peaks that are hard to explain with a single luminosity source at the center and prefer the existence of a complicated dense CSM structure. The “spiky” bolometric LC of SN 2017egm is also suggests an interaction model (Wheeler et al 2017). The LC modulations observed in some SLSNe Ic are also likely to indicate the existence of an outer energy source like a dense CSM. Even if there is a major central power source like a magnetar powering a SLSN Ic LC, some dense CSM that has a minor contribution to the luminosity may also exist. A combination of central and outer powering sources could better explain the general SLSN Ic LCs.

Multi-frequency studies of SLSNe Ic are helpful in distinguishing the different powering mechanisms. For example, the magnetar model predicts a late-phase increase in X-rays at the “ionization breakout” (Metzger et al 2014), while X-rays in the interaction model are expected in some cases after the shock breakout stage that lasts a few months. Margutti et al (2017) report their observational efforts to detect SLSNe in X-rays but only a few detections are obtained so far and it is still hard to distinguish the powering mechanisms in this way. Tolstov et al (2017b) recently suggested that the ultraviolet luminosity could be better explained by the interaction model. It is not totally clear yet if the ultraviolet luminosities are the decisive distinguisher among the models, given the uncertainties in how magnetars transform their spin energy to the surrounding ejecta. More studies are required in this regard. No γ -ray detections from SLSNe could indicate that the magnetic field strengths in the compact remnants of SLSNe are much less than required to power the LCs (Renault-Tinacci et al 2017).

The precursors found in many SLSNe Ic are hard to explain with any model. If the precursor is from the shock breakout, the progenitor radii need to be more than $500 R_{\odot}$ with a reasonable assumption of the explosion energy (Nicholl et al 2015b, Piro 2015). These huge radii are unexpected in hydrogen-free progenitors and some mechanisms to make an extended envelope are required. The ^{56}Ni -powered model only has the central heating source without much hydrodynamical effect and such extended envelopes are necessary to explain the precursor.

The CSM interaction and magnetar models are able to explain the precursor without invoking the extremely extended progenitor for SLSNe Ic. For the CSM interaction model, Moriya and Maeda (2012) illustrate that the precursor bump can be naturally made by the ionization change in the massive CSM to power the major LCs in SLSNe Ic. Regardless of the luminosity source of the precursor, the precursor LC bump can be made by the massive CSM required to explain the main peak of SLSN Ic LCs. In the magnetar-powered model, so-called “magnetar shock breakout” can occur in the ejecta, making a precursor on some occasions (Kasen et al 2016, see also Section 5). When a huge magnetar rotational energy is released near the center of an exploding star, another shock wave can be launched. If the shock becomes strong enough to be a radiation-dominated shock, another

shock breakout can occur when the shock reaches the surface of the ejecta resulting in a precursor bump observed in SLSNe Ic. However, in 1D LC simulations, the shock breakout bump is usually not clearly seen as observed unless the central heating efficiency is artificially reduced (Kasen et al 2016, Moriya et al 2016). More studies are needed to see if the magnetar shock breakout can generally explain the precursors.

6.2 Spectra

Spectra of SLSNe Ic provides plenty of information to distinguish the powering mechanisms. The ^{56}Ni -power model is generally less favored recently because of the lack of strong Fe absorptions and emissions in SLSNe Ic (e.g., Jerkstrand et al 2017, see also Section 3). The models with a central engine like magnetars are generally found to match the spectra well (e.g., Mazzali et al 2016, Dessart et al 2012). SLSNe Ic do not show narrow features that are found in less luminous Type Ib (e.g., Pastorello et al 2016) and Type Ic (e.g., Ben-Ami et al 2014) SNe with strong CSM interactions. There are some suggested mechanisms to hide the possible narrow lines in the interacting SNe (e.g., Chevalier and Irwin 2011, Moriya and Tominaga 2012), but they may not generally occur. Spectral modeling is required to judge if the lack of the narrow emissions in SLSNe Ic is consistent with the interaction model.

Chen et al (2017a) performed a detailed spectral modeling of the Type Ic SLSN LSQ14mo. They show that its line features did not change for a while but the continuum significantly changed in the same period. The temperature deduced from the line features does not match that deduced from the continuum for some period. In their interpretation, the continuum may be affected by an external heating source like CSM interaction in addition to a central heating source like a magnetar that is determining the temperature of the line forming region in the SN ejecta. This indicates that more than a single energy source is responsible for the LCs for all the periods. Different powering sources could be contributing at the same time to power SLSNe. Another example of this kind is Gaia16apd, which is suggested to be powered by a combination of CSM interaction and ^{56}Ni heating (Tolstov et al 2017b). ^{56}Ni heating may contribute to SLSNe IIn in addition to CSM interaction if a significant amount of ^{56}Ni is produced, although CSM interaction by itself can explain SN 2006gy (Miller et al 2010).

7 Other models

Several other ideas have been raised as the power sources of SLSNe. For example, the fallback accretion onto the central compact remnant of the exploding stars can potentially release a sufficient energy to power SLSNe (Dexter and Kasen 2013). It is also suggested that a latent heat released by the phase transition from neutron stars to quark stars is sufficient to power SLSNe (e.g., Ouyed et al 2012).

It is possible that not a single energy source is playing a role in powering SLSNe. Two or more energy sources can provide heat sources at the same time.

We also need to keep in mind the possibility that none of the energy sources currently proposed are correct – a power source that is completely missed so far may still exist.

Acknowledgements This review made use of the Weizmann interactive supernova data repository - <http://wiserep.weizmann.ac.il> (Yaron and Gal-Yam 2012) and the Open Supernova Catalog - <https://sne.space/> (Guillochon et al 2017). TJM is supported by the Grants-in-Aid for Scientific Research of the Japan Society for the Promotion of Science (16H07413, 17H02864) and the Munich Institute for Astro- and Particle Physics (MIAPP) of the DFG cluster of excellence "Origin and Structure of the Universe." The work of ES (interaction models) is supported by the Russian Scientific Foundation grant 16-12-10519. RAC was supported in part by NASA grant NNX12AF90G.

References

- Agnoletto I, Benetti S, Cappellaro E, Zampieri L, Turatto M, Mazzali P, Pastorello A, Della Valle M, Bufano F, Harutyunyan A, Navasardyan H, Elias-Rosa N, Taubenberger S, Spiro S, Valenti S (2009) SN 2006gy: Was it Really Extraordinary? *Astrophys.J.* 691:1348–1359, DOI 10.1088/0004-637X/691/2/1348, 0810.0635
- Angus CR, Levan AJ, Perley DA, Tanvir NR, Lyman JD, Stanway ER, Fruchter AS (2016) A Hubble Space Telescope survey of the host galaxies of Superluminous Supernovae. *M.N.R.A.S.* 458:84–104, DOI 10.1093/mnras/stw063, 1601.01874
- Arcavi I, Wolf WM, Howell DA, Bildsten L, Leloudas G, Hardin D, Prajs S, Perley DA, Svirski G, Gal-Yam A, Katz B, McCully C, Cenko SB, Lidman C, Sullivan M, Valenti S, Astier P, Balland C, Carlberg RG, Conley A, Fouchez D, Guy J, Pain R, Palanque-Delabrouille N, Perrett K, Pritchett CJ, Regnault N, Rich J, Ruhlmann-Kleider V (2016) Rapidly Rising Transients in the Supernova–Superluminous Supernova Gap. *Astrophys.J.* 819:35, DOI 10.3847/0004-637X/819/1/35, 1511.00704
- Arnett D (1996) *Supernovae and Nucleosynthesis: An Investigation of the History of Matter from the Big Bang to the Present*
- Arnett WD (1980) Analytic solutions for light curves of supernovae of Type II. *Astrophys.J.* 237:541–549, DOI 10.1086/157898
- Arnett WD (1982) Type I supernovae. I - Analytic solutions for the early part of the light curve. *Astrophys.J.* 253:785–797, DOI 10.1086/159681
- Axelrod TS (1980) Late time optical spectra from the Ni-56 model for Type 1 supernovae. PhD thesis, California Univ., Santa Cruz.
- Barbary K, Dawson KS, Tokita K, Aldering G, Amanullah R, Connolly NV, Doi M, Faccioli L, Fadeyev V, Fruchter AS, Goldhaber G, Goobar A, Gude A, Huang X, Ihara Y, Konishi K, Kowalski M, Lidman C, Meyers J, Morokuma T, Nugent P, Perlmutter S, Rubin D, Schlegel D, Spadafora AL, Suzuki N, Swift HK, Takahashi N, Thomas RC, Yasuda N (2009) Discovery of an Unusual Optical Transient with the Hubble Space Telescope. *Astrophys.J.* 690:1358–1362, DOI 10.1088/0004-637X/690/2/1358, 0809.1648
- Barkat Z, Rakavy G, Sack N (1967) Dynamics of Supernova Explosion Resulting from Pair Formation. *Physical Review Letters* 18:379–381, DOI 10.1103/PhysRevLett.18.379
- Ben-Ami S, Gal-Yam A, Mazzali PA, Gnat O, Modjaz M, Rabinak I, Sullivan M, Bildsten L, Poznanski D, Yaron O, Arcavi I, Bloom JS, Horesh A, Kasliwal MM, Kulkarni SR, Nugent PE, Ofek EO, Perley D, Quimby R, Xu D (2014) SN 2010mb: Direct Evidence for a Supernova Interacting with a Large

- Amount of Hydrogen-free Circumstellar Material. *Astrophys.J.* 785:37, DOI 10.1088/0004-637X/785/1/37, 1309.6496
- Benetti S, Nicholl M, Cappellaro E, Pastorello A, Smartt SJ, Elias-Rosa N, Drake AJ, Tomasella L, Turatto M, Harutyunyan A, Taubenberger S, Hachinger S, Morales-Garoffolo A, Chen TW, Djorgovski SG, Fraser M, Gal-Yam A, Inserra C, Mazzali P, Pumo ML, Sollerman J, Valenti S, Young DR, Dennefeld M, Le Guillou L, Fleury M, Léget PF (2014) The supernova CSS121015:004244+132827: a clue for understanding superluminous supernovae. *M.N.R.A.S.* 441:289–303, DOI 10.1093/mnras/stu538, 1310.1311
- Berger E, Chornock R, Lunnan R, Foley R, Czekala I, Rest A, Leibler C, Soderberg AM, Roth K, Narayan G, Huber ME, Milisavljevic D, Sanders NE, Drout M, Margutti R, Kirshner RP, Marion GH, Challis PJ, Riess AG, Smartt SJ, Burgett WS, Hodapp KW, Heasley JN, Kaiser N, Kudritzki RP, Magnier EA, McCrum M, Price PA, Smith K, Tonry JL, Wainscoat RJ (2012) Ultraluminous Supernovae as a New Probe of the Interstellar Medium in Distant Galaxies. *Astrophys.J.Lett.* 755:L29, DOI 10.1088/2041-8205/755/2/L29, 1206.4050
- Bersten MC, Benvenuto OG, Orellana M, Nomoto K (2016) The Unusual Superluminous Supernovae SN 2011kl and ASASSN-15lh. *Astrophys.J.Lett.* 817:L8, DOI 10.3847/2041-8205/817/1/L8, 1601.01021
- Blanchard PK, Nicholl M, Berger E, Guillochon J, Margutti R, Chornock R, Alexander KD, Leja J, Drout MR (2017) PS16dtm: A Tidal Disruption Event in a Narrow-line Seyfert 1 Galaxy. *Astrophys.J.* 843:106, DOI 10.3847/1538-4357/aa77f7, 1703.07816
- Blinnikov S (2016) Radiative shock waves and their role in solving puzzles of Superluminous Supernovae. *ArXiv e-prints* 1611.00513
- Blinnikov SI, Eastman R, Bartunov OS, Popolitov VA, Woosley SE (1998) A Comparative Modeling of Supernova 1993J. *Astrophys.J.* 496:454–472, DOI 10.1086/305375, astro-ph/9711055
- Blinnikov SI, Röpke FK, Sorokina EI, Gieseler M, Reinecke M, Travaglio C, Hillebrandt W, Stritzinger M (2006) Theoretical light curves for deflagration models of type Ia supernova. *Astron.Astrophys.* 453:229–240, DOI 10.1051/0004-6361:20054594, astro-ph/0603036
- Blondin JM, Chevalier RA (2017) Pulsar Wind Bubble Blowout from a Supernova. *Astrophys.J.* 845:139, DOI 10.3847/1538-4357/aa8267, 1707.07021
- Blondin JM, Chevalier RA, Frierson DM (2001) Pulsar Wind Nebulae in Evolved Supernova Remnants. *Astrophys.J.* 563:806–815, DOI 10.1086/324042, astro-ph/0107076
- Bose S, Dong S, Pastorello A, Filippenko AV, Kochanek CS, Mauerhan J, Romero-Cañizales C, Brink TG, Chen P, Prieto JL, Post R, Ashall C, Grupe D, Tomasella L, Benetti S, Shappee BJ, Stanek KZ, Cai Z, Falco E, Lundqvist P, Mattila S, Mutel R, Ochner P, Pooley D, Stritzinger MD, Villanueva S Jr, Zheng W, Beswick RJ, Brown PJ, Cappellaro E, Davis S, Fraser M, de Jaeger T, Elias-Rosa N, Gall C, Gaudi BS, Herczeg GJ, Hestenes J, Holoien TWS, Hosseinzadeh G, Hsiao EY, Hu S, Jaejin S, Jeffers B, Koff RA, Kumar S, Kurtenkov A, Lau MW, Prentice S, Reynolds T, Rudy RJ, Shahbandeh M, Somero A, Stassun KG, Thompson TA, Valenti S, Woo JH, Yunus S (2018) Gaia17biu/SN 2017egm in NGC 3191: The Closest Hydrogen-poor Superluminous Supernova to Date Is in a Normal, Massive, Metal-rich Spiral Galaxy. *Astrophys.J.* 853:57, DOI 10.3847/1538-4357/aaa298, 1708.00864
- Bucciantini N, Amato E, Bandiera R, Blondin JM, Del Zanna L (2004) Magnetic Rayleigh-Taylor instability for Pulsar Wind Nebulae in expanding Supernova Remnants. *Astron.Astrophys.* 423:253–265, DOI 10.1051/0004-6361:20040360, astro-ph/0405276
- Chandra P (2018) Circumstellar Interaction in Supernovae in Dense Environments – An Observational Perspective. *Space Sci. Rev.* 214:27, DOI 10.1007/s11214-017-0461-6, 1712.07405
- Chatzopoulos E, Wheeler JC (2012) Effects of Rotation on the Minimum Mass of Primordial Progenitors of Pair-instability Supernovae. *Astrophys.J.* 748:42, DOI 10.1088/0004-637X/748/1/42, 1201.1328

-
- Chatzopoulos E, Wheeler JC, Vinko J (2012) Generalized Semi-analytical Models of Supernova Light Curves. *Astrophys.J.* 746:121, DOI 10.1088/0004-637X/746/2/121, 1111.5237
- Chatzopoulos E, Wheeler JC, Vinko J, Horvath ZL, Nagy A (2013) Analytical Light Curve Models of Superluminous Supernovae: χ^2 -minimization of Parameter Fits. *Astrophys.J.* 773:76, DOI 10.1088/0004-637X/773/1/76, 1306.3447
- Chatzopoulos E, van Rossum DR, Craig WJ, Whalen DJ, Smidt J, Wiggins B (2015) Emission from Pair-instability Supernovae with Rotation. *Astrophys.J.* 799:18, DOI 10.1088/0004-637X/799/1/18, 1410.0039
- Chen KJ, Heger A, Woosley S, Almgren A, Whalen DJ (2014) Pair Instability Supernovae of Very Massive Population III Stars. *Astrophys.J.* 792:44, DOI 10.1088/0004-637X/792/1/44, 1402.5960
- Chen KJ, Woosley SE, Sukhbold T (2016) Magnetar-Powered Supernovae in Two Dimensions. I. Superluminous Supernovae. *Astrophys.J.* 832:73, DOI 10.3847/0004-637X/832/1/73, 1604.07989
- Chen TW, Smartt SJ, Bresolin F, Pastorello A, Kudritzki RP, Kotak R, McCrum M, Fraser M, Valenti S (2013) The Host Galaxy of the Super-luminous SN 2010gx and Limits on Explosive ^{56}Ni Production. *Astrophys.J.Lett.* 763:L28, DOI 10.1088/2041-8205/763/2/L28, 1210.4027
- Chen TW, Smartt SJ, Jerkstrand A, Nicholl M, Bresolin F, Kotak R, Polshaw J, Rest A, Kudritzki R, Zheng Z, Elias-Rosa N, Smith K, Inserra C, Wright D, Kankare E, Kangas T, Fraser M (2015) The host galaxy and late-time evolution of the superluminous supernova PTF12dam. *M.N.R.A.S.* 452:1567–1586, DOI 10.1093/mnras/stv1360, 1409.7728
- Chen TW, Nicholl M, Smartt SJ, Mazzali PA, Yates RM, Moriya TJ, Inserra C, Langer N, Krühler T, Pan YC, Kotak R, Galbany L, Schady P, Wiseman P, Greiner J, Schulze S, Man AWS, Jerkstrand A, Smith KW, Dennefeld M, Baltay C, Bolmer J, Kankare E, Knust F, Maguire K, Rabinowitz D, Rostami S, Sullivan M, Young DR (2017a) The evolution of superluminous supernova LSQ14mo and its interacting host galaxy system. *Astron.Astrophys.* 602:A9, DOI 10.1051/0004-6361/201630163, 1611.09910
- Chen TW, Schady P, Xiao L, Eldridge JJ, Schweyer T, Lee CH, Yu PC, Smartt SJ, Inserra C (2017b) Spatially Resolved MaNGA Observations of the Host Galaxy of Superluminous Supernova 2017egm. *Astrophys.J.Lett.* 849:L4, DOI 10.3847/2041-8213/aa8f40, 1708.04618
- Chen TW, Smartt SJ, Yates RM, Nicholl M, Krühler T, Schady P, Dennefeld M, Inserra C (2017c) Superluminous supernova progenitors have a half-solar metallicity threshold. *M.N.R.A.S.* 470:3566–3573, DOI 10.1093/mnras/stx1428, 1605.04925
- Chevalier RA (1977) Was SN 1054 A Type II Supernova? In: Schramm DN (ed) *Supernovae, Astrophysics and Space Science Library*, vol 66, p 53, DOI 10.1007/978-94-010-1229-4_5
- Chevalier RA (2005) Young Core-Collapse Supernova Remnants and Their Supernovae. *Astrophys.J.* 619:839–855, DOI 10.1086/426584, astro-ph/0409013
- Chevalier RA, Fransson C (2003) Supernova Interaction with a Circumstellar Medium. In: Weiler K (ed) *Supernovae and Gamma-Ray Bursters, Lecture Notes in Physics*, Berlin Springer Verlag, vol 598, pp 171–194, DOI 10.1007/3-540-45863-8_10, astro-ph/0110060
- Chevalier RA, Irwin CM (2011) Shock Breakout in Dense Mass Loss: Luminous Supernovae. *Astrophys.J.Lett.* 729:L6, DOI 10.1088/2041-8205/729/1/L6, 1101.1111
- Chevalier RA, Soker N (1989) Asymmetric envelope expansion of supernova 1987A. *Astrophys.J.* 341:867–882, DOI 10.1086/167545
- Chomiuk L, Chornock R, Soderberg AM, Berger E, Chevalier RA, Foley RJ, Huber ME, Narayan G, Rest A, Gezari S, Kirshner RP, Riess A, Rodney SA, Smartt SJ, Stubbs CW, Tonry JL, Wood-Vasey WM, Burgett WS, Chambers KC, Czekala I, Flewelling H, Forster K, Kaiser N, Kudritzki RP, Magnier EA, Martin DC, Morgan JS, Neill JD, Price PA, Roth KC, Sanders NE, Wainscoat RJ (2011) Pan-STARRS1 Discovery of Two Ultraluminous Supernovae at $z \simeq 0.9$.

- Astrophys.J. 743:114, DOI 10.1088/0004-637X/743/2/114, 1107.3552
- Cikota A, De Cia A, Schulze S, Vreeswijk PM, Leloudas G, Gal-Yam A, Perley DA, Cikota S, Kim S, Patat F, Lunnan R, Quimby R, Yaron O, Yan L, Mazzali PA (2017) Spatially resolved analysis of superluminous supernovae PTF 11hrq and PTF 12dam host galaxies. *M.N.R.A.S.* 469:4705–4717, DOI 10.1093/mnras/stx1110, 1705.01948
- Cooke J, Sullivan M, Gal-Yam A, Barton EJ, Carlberg RG, Ryan-Weber EV, Horst C, Omori Y, Díaz CG (2012) Superluminous supernovae at redshifts of 2.05 and 3.90. *Nature* 491:228–231, DOI 10.1038/nature11521, 1211.2003
- Coppejans DL, Margutti R, Guidorzi C, Chomiuk L, Alexander KD, Berger E, Bietenholz MF, Blanchard PK, Challis P, Chornock R, Drout M, Fong W, Mac Fadyen A, Migliori G, Milisavljevic D, Nicholl M, Parrent JT, Terreran G, Zauderer BA (2017) Jets in Hydrogen-poor Super-luminous Supernovae: Constraints from a Comprehensive Analysis of Radio Observations. ArXiv e-prints 1711.03428
- Curtin C, Cooke J, Moriya TJ, Bernard SR, Galbany L, Jiang Ja, Lee CH, Maeda K, Morokuma T, Nomoto K, Pignata G, Pritchard T, Quimby RM, Suzuki N, Takahashi I, Tanaka M, Tanaka M, Tominaga N, Yamaguchi M, Yasuda N (2018) First release of high-redshift superluminous supernovae from the Subaru High-Z sUpernova Campaign (SHIZUCA). II. Spectroscopic properties. ArXiv e-prints 1801.08241
- da Cruz MT, Chan Y, Larimer RM, Lesko KT, Norman EB, Stokstad RG, Wietfeldt FE, Žlimen I (1992) Half-life of ^{56}Ni . *Phys.Rev.C* 46:1132–1135, DOI 10.1103/PhysRevC.46.1132
- De Cia A, Gal-Yam A, Rubin A, Leloudas G, Vreeswijk P, Perley DA, Quimby R, Yan L, Sullivan M, Flörs A, Sollerman J, Bersier D, Cenko SB, Gal-Yam M, Maguire K, Ofek EO, Prentice S, Schulze S, Spyromilio J, Valenti S, Arcavi I, Corsi A, Howell A, Mazzali P, Kasliwal MM, Taddia F, Yaron O (2017) Light curves of hydrogen-poor Superluminous Supernovae from the Palomar Transient Factory. ArXiv e-prints 1708.01623
- Dessart L, Hillier DJ, Waldman R, Livne E, Blondin S (2012) Superluminous supernovae: ^{56}Ni power versus magnetar radiation. *M.N.R.A.S.* 426:L76–L80, DOI 10.1111/j.1745-3933.2012.01329.x, 1208.1214
- Dessart L, Waldman R, Livne E, Hillier DJ, Blondin S (2013) Radiative properties of pair-instability supernova explosions. *M.N.R.A.S.* 428:3227–3251, DOI 10.1093/mnras/sts269, 1210.6163
- Dessart L, Audit E, Hillier DJ (2015) Numerical simulations of superluminous supernovae of type IIn. *M.N.R.A.S.* 449:4304–4325, DOI 10.1093/mnras/stv609, 1503.05463
- Dexter J, Kasen D (2013) Supernova Light Curves Powered by Fallback Accretion. *Astrophys.J.* 772:30, DOI 10.1088/0004-637X/772/1/30, 1210.7240
- Dong S, Shappee BJ, Prieto JL, Jha SW, Stanek KZ, Holoiem TWS, Kochanek CS, Thompson TA, Morrell N, Thompson IB, Basu U, Beacom JF, Bersier D, Brimacombe J, Brown JS, Bufano F, Chen P, Conseil E, Danilet AB, Falco E, Grupe D, Kiyota S, Masi G, Nicholls B, Olivares E F, Pignata G, Pojmanski G, Simonian GV, Szczygiel DM, Woźniak PR (2016) ASASSN-15lh: A highly super-luminous supernova. *Science* 351:257–260, DOI 10.1126/science.aac9613, 1507.03010
- Drake AJ, Djorgovski SG, Prieto JL, Mahabal A, Balam D, Williams R, Graham MJ, Catelan M, Beshore E, Larson S (2010) Discovery of the Extremely Energetic Supernova 2008fz. *Astrophys.J.Lett.* 718:L127–L131, DOI 10.1088/2041-8205/718/2/L127, 0908.1990
- Drake AJ, Djorgovski SG, Mahabal A, Anderson J, Roy R, Mohan V, Ravindranath S, Frail D, Gezari S, Neill JD, Ho LC, Prieto JL, Thompson D, Thorstensen J, Wagner M, Kowalski R, Chiang J, Grove JE, Schinzel FK, Wood DL, Carrasco L, Recillas E, Kewley L, Archana KN, Basu A, Wadadekar Y, Kumar B, Myers AD, Phinney ES, Williams R, Graham MJ, Catelan M, Beshore E, Larson S, Christensen E (2011) The Discovery and Nature of the Optical Transient CSS100217:102913+404220. *Astrophys.J.* 735:106, DOI

- 10.1088/0004-637X/735/2/106, 1103.5514
- Drout MR, Soderberg AM, Gal-Yam A, Cenko SB, Fox DB, Leonard DC, Sand DJ, Moon DS, Arcavi I, Green Y (2011) The First Systematic Study of Type Ibc Supernova Multi-band Light Curves. *Astrophys.J.* 741:97, DOI 10.1088/0004-637X/741/2/97, 1011.4959
- Espinoza CM, Lyne AG, Stappers BW (2017) New long-term braking index measurements for glitching pulsars using a glitch-template method. *M.N.R.A.S.* 466:147–162, DOI 10.1093/mnras/stw3081, 1611.08314
- Falk SW, Arnett WD (1977) Radiation Dynamics, Envelope Ejection, and Supernova Light Curves. *Astrophys.J.Supp.* 33:515, DOI 10.1086/190440
- Fransson C, Ergon M, Challis PJ, Chevalier RA, France K, Kirshner RP, Marion GH, Milisavljevic D, Smith N, Bufano F, Friedman AS, Kangas T, Larsson J, Mattila S, Benetti S, Chornock R, Czekala I, Soderberg A, Sollerman J (2014) High-density Circumstellar Interaction in the Luminous Type II_n SN 2010jl: The First 1100 Days. *Astrophys.J.* 797:118, DOI 10.1088/0004-637X/797/2/118, 1312.6617
- Funck E, Schötzig U, Woods MJ, Sephton JP, Munster AS, Dean JCJ, Blanchis P, Chauvenet B (1992) ⁵⁶Co standardization and half-life. *Nuclear Instruments and Methods in Physics Research A* 312:334–338, DOI 10.1016/0168-9002(92)90177-6
- Gaffet B (1977) Pulsar theory of supernova light curves. I - Dynamical effect and thermalization of the pulsar strong waves. *Astrophys.J.* 216:565–577, DOI 10.1086/155498
- Gal-Yam A (2012) Luminous Supernovae. *Science* 337:927, DOI 10.1126/science.1203601, 1208.3217
- Gal-Yam A, Mazzali P, Ofek EO, Nugent PE, Kulkarni SR, Kasliwal MM, Quimby RM, Filippenko AV, Cenko SB, Chornock R, Waldman R, Kasen D, Sullivan M, Beshore EC, Drake AJ, Thomas RC, Bloom JS, Poznanski D, Miller AA, Foley RJ, Silverman JM, Arcavi I, Ellis RS, Deng J (2009) Supernova 2007bi as a pair-instability explosion. *Nature* 462:624–627, DOI 10.1038/nature08579, 1001.1156
- Gänsicke BT, Levan AJ, Marsh TR, Wheatley PJ (2009) SCP 06F6: A Carbon-rich Extragalactic Transient at Redshift $z \sim 0.14$? *Astrophys.J.Lett.* 697:L129–L132, DOI 10.1088/0004-637X/697/2/L129, 0809.2562
- Georgy C, Meynet G, Ekström S, Wade GA, Petit V, Keszthelyi Z, Hirschi R (2017) Possible pair-instability supernovae at solar metallicity from magnetic stellar progenitors. *Astron.Astrophys.* 599:L5, DOI 10.1051/0004-6361/201730401, 1702.02340
- Gezari S, Halpern JP, Grupe D, Yuan F, Quimby R, McKay T, Chamorro D, Sisson MD, Akerlof C, Wheeler JC, Brown PJ, Cenko SB, Rau A, Djordjevic JO, Terndrup DM (2009) Discovery of the Ultra-Bright Type II-L Supernova 2008es. *Astrophys.J.* 690:1313–1321, DOI 10.1088/0004-637X/690/2/1313, 0808.2812
- Gilkis A, Soker N, Papish O (2016) Explaining the Most Energetic Supernovae with an Inefficient Jet-feedback Mechanism. *Astrophys.J.* 826:178, DOI 10.3847/0004-637X/826/2/178, 1511.01471
- Gilmer MS, Kozyreva A, Hirschi R, Fröhlich C, Yusof N (2017) Pair-instability Supernova Simulations: Progenitor Evolution, Explosion, and Light Curves. *Astrophys.J.* 846:100, DOI 10.3847/1538-4357/aa8461, 1706.07454
- Ginzburg S, Balberg S (2012) Superluminous Light Curves from Supernovae Exploding in a Dense Wind. *Astrophys.J.* 757:178, DOI 10.1088/0004-637X/757/2/178, 1205.3455
- Grasberg EK, Nadyozhin DK (1987) The onset of a type II supernova outburst in a circumstellar envelope created by the intense stellar wind from the presupernova. *Astron.Zh.* 64:1199–1209
- Grasberg EK, Imshenik VS, Nadyozhin DK (1971) On the Theory of the Light Curves of Supernovae (In Russian). *Astrophys.Sp.Sc.* 10:3, DOI 10.1007/BF00654603
- Greiner J, Mazzali PA, Kann DA, Krühler T, Pian E, Prentice S, Olivares E F, Rossi A, Klose S, Taubenberger S, Knust F, Afonso PMJ, Ashall C, Bolmer J,

- Delvaux C, Diehl R, Elliott J, Filgas R, Fynbo JPU, Graham JF, Guelbenzu AN, Kobayashi S, Leloudas G, Savaglio S, Schady P, Schmidl S, Schweyer T, Sudilovsky V, Tanga M, Updike AC, van Eerten H, Varela K (2015) A very luminous magnetar-powered supernova associated with an ultra-long γ -ray burst. *Nature* 523:189–192, DOI 10.1038/nature14579, 1509.03279
- Guillochon J, Parrent J, Kelley LZ, Margutti R (2017) An Open Catalog for Supernova Data. *Astrophys.J.* 835:64, DOI 10.3847/1538-4357/835/1/64, 1605.01054
- Heger A, Woosley SE (2002) The Nucleosynthetic Signature of Population III. *Astrophys.J.* 567:532–543, DOI 10.1086/338487, astro-ph/0107037
- Howell DA (2017) *Superluminous Supernovae*. Springer International Publishing, Cham, pp 1–29. DOI 10.1007/978-3-319-20794-0_41-1, URL http://dx.doi.org/10.1007/978-3-319-20794-0_41-1
- Howell DA, Kasen D, Lidman C, Sullivan M, Conley A, Astier P, Balland C, Carlberg RG, Fouchez D, Guy J, Hardin D, Pain R, Palanque-Delabrouille N, Perrett K, Pritchett CJ, Regnault N, Rich J, Ruhlmann-Kleider V (2013) Two Superluminous Supernovae from the Early Universe Discovered by the Supernova Legacy Survey. *Astrophys.J.* 779:98, DOI 10.1088/0004-637X/779/2/98, 1310.0470
- Inserra C, Smartt SJ (2014) Superluminous Supernovae as Standardizable Candles and High-redshift Distance Probes. *Astrophys.J.* 796:87, DOI 10.1088/0004-637X/796/2/87, 1409.4429
- Inserra C, Smartt SJ, Jerkstrand A, Valenti S, Fraser M, Wright D, Smith K, Chen TW, Kotak R, Pastorello A, Nicholl M, Bresolin F, Kudritzki RP, Benetti S, Botticella MT, Burgett WS, Chambers KC, Ergon M, Flewelling H, Fynbo JPU, Geier S, Hodapp KW, Howell DA, Huber M, Kaiser N, Leloudas G, Magill L, Magnier EA, McCrum MG, Metcalfe N, Price PA, Rest A, Sollerman J, Sweeney W, Taddia F, Taubenberger S, Tonry JL, Wainscoat RJ, Waters C, Young D (2013) Super-luminous Type Ic Supernovae: Catching a Magnetar by the Tail. *Astrophys.J.* 770:128, DOI 10.1088/0004-637X/770/2/128, 1304.3320
- Inserra C, Bulla M, Sim SA, Smartt SJ (2016) Spectropolarimetry of Superluminous Supernovae: Insight into Their Geometry. *Astrophys.J.* 831:79, DOI 10.3847/0004-637X/831/1/79, 1607.02353
- Inserra C, Nicholl M, Chen TW, Jerkstrand A, Smartt SJ, Krühler T, Anderson JP, Baltay C, Della Valle M, Fraser M, Gal-Yam A, Galbany L, Kankare E, Maguire K, Rabinowitz D, Smith K, Valenti S, Young DR (2017) Complexity in the light curves and spectra of slow-evolving superluminous supernovae. *M.N.R.A.S.* 468:4642–4662, DOI 10.1093/mnras/stx834, 1701.00941
- Inserra C, Nichol RC, Scovaccicchi D, Amiaux J, Brescia M, Burigana C, Cappellaro E, Carvalho CS, Cavuoti S, Conforti V, Cuillandre JC, da Silva A, De Rosa A, Della Valle M, Dinis J, Franceschi E, Hook I, Hudelot P, Jahnke K, Kitching T, Kurki-Suonio H, Lloro I, Longo G, Maiorano E, Maris M, Rhodes JD, Scaramella R, Smartt SJ, Sullivan M, Tao C, Toledo-Moreo R, Tereno I, Trifoglio M, Valenziano L (2018a) Euclid: Superluminous supernovae in the Deep Survey. *Astron.Astrophys.* 609:A83, DOI 10.1051/0004-6361/201731758, 1710.09585
- Inserra C, Smartt SJ, Gall EEE, Leloudas G, Chen TW, Schulze S, Jerkstrand A, Nicholl M, Anderson JP, Arcavi I, Benetti S, Cartier RA, Childress M, Della Valle M, Flewelling H, Fraser M, Gal-Yam A, Gutiérrez CP, Hosseinzadeh G, Howell DA, Huber M, Kankare E, Krühler T, Magnier EA, Maguire K, McCully C, Prajs S, Primak N, Scalzo R, Schmidt BP, Smith M, Smith KW, Tucker BE, Valenti S, Wilman M, Young DR, Yuan F (2018b) On the nature of hydrogen-rich superluminous supernovae. *M.N.R.A.S.* 475:1046–1072, DOI 10.1093/mnras/stx3179, 1604.01226
- Izzo L, Thöne CC, García-Benito R, de Ugarte Postigo A, Cano Z, Kann DA, Bensch K, Della Valle M, Galadí-Enríquez D, Hedrosa RP (2018) The host of the Type I SLSN 2017egm. A young, sub-solar metallicity environment in a massive spiral galaxy. *Astron.Astrophys.* 610:A11, DOI 10.1051/0004-6361/201731766, 1708.03856

- Japelj J, Vergani SD, Salvaterra R, Hunt LK, Mannucci F (2016) Taking stock of superluminous supernovae and long gamma-ray burst host galaxy comparison using a complete sample of LGRBs. *Astron.Astrophys.* 593:A115, DOI 10.1051/0004-6361/201628603, 1607.01045
- Jerkstrand A, Smartt SJ, Heger A (2016) Nebular spectra of pair-instability supernovae. *M.N.R.A.S.* 455:3207–3229, DOI 10.1093/mnras/stv2369, 1510.02698
- Jerkstrand A, Smartt SJ, Inserra C, Nicholl M, Chen TW, Krühler T, Sollerman J, Taubenberger S, Gal-Yam A, Kankare E, Maguire K, Fraser M, Valenti S, Sullivan M, Cartier R, Young DR (2017) Long-duration Superluminous Supernovae at Late Times. *Astrophys.J.* 835:13, DOI 10.3847/1538-4357/835/1/13, 1608.02994
- Jogerst CC, Whalen DJ (2011) The Early Evolution of Primordial Pair-instability Supernovae. *Astrophys.J.* 728:129, DOI 10.1088/0004-637X/728/2/129, 1010.4360
- Kankare E, Kotak R, Mattila S, Lundqvist P, Ward MJ, Fraser M, Lawrence A, Smartt SJ, Meikle WPS, Bruce A, Harmanen J, Hutton SJ, Inserra C, Kangas T, Pastorello A, Reynolds T, Romero-Cañizales C, Smith KW, Valenti S, Chambers KC, Hodapp KW, Huber ME, Kaiser N, Kudritzki RP, Magnier EA, Tonry JL, Wainscoat RJ, Waters C (2017) A population of highly energetic transient events in the centres of active galaxies. *Nature Astronomy* 1:865–871, DOI 10.1038/s41550-017-0290-2, 1711.04577
- Kasen D, Bildsten L (2010) Supernova Light Curves Powered by Young Magnetars. *Astrophys.J.* 717:245–249, DOI 10.1088/0004-637X/717/1/245, 0911.0680
- Kasen D, Woosley SE, Heger A (2011) Pair Instability Supernovae: Light Curves, Spectra, and Shock Breakout. *Astrophys.J.* 734:102, DOI 10.1088/0004-637X/734/2/102, 1101.3336
- Kasen D, Metzger BD, Bildsten L (2016) Magnetar-driven Shock Breakout and Double-peaked Supernova Light Curves. *Astrophys.J.* 821:36, DOI 10.3847/0004-637X/821/1/36, 1507.03645
- Kawabata KS, Tanaka M, Maeda K, Hattori T, Nomoto K, Tominaga N, Yamanaka M (2009) Extremely Luminous Supernova 2006gy at Late Phase: Detection of Optical Emission from Supernova. *Astrophys.J.* 697:747–757, DOI 10.1088/0004-637X/697/1/747, 0902.1440
- Knop R, Aldering G, Deustua S, Goldhaber G, Kim M, Nugent P, Helin E, Pravdo S, Rabinowitz D, Lawrence K (1999) Supernovae 1999as and 1999at in Anonymous Galaxies. *IAU Circ.* 7128
- Kotera K, Phinney ES, Olinto AV (2013) Signatures of pulsars in the light curves of newly formed supernova remnants. *M.N.R.A.S.* 432:3228–3236, DOI 10.1093/mnras/stt680, 1304.5326
- Kozyreva A, Blinnikov S (2015) Can pair-instability supernova models match the observations of superluminous supernovae? *M.N.R.A.S.* 454:4357–4365, DOI 10.1093/mnras/stv2287, 1510.00439
- Kozyreva A, Blinnikov S, Langer N, Yoon SC (2014) Observational properties of low-redshift pair instability supernovae. *Astron.Astrophys.* 565:A70, DOI 10.1051/0004-6361/201423447, 1403.5212
- Kozyreva A, Gilmer M, Hirschi R, Fröhlich C, Blinnikov S, Wollaeger RT, Noebauer UM, van Rossum DR, Heger A, Even WP, Waldman R, Tolstov A, Chatzopoulos E, Sorokina E (2017) Fast evolving pair-instability supernova models: evolution, explosion, light curves. *M.N.R.A.S.* 464:2854–2865, DOI 10.1093/mnras/stw2562, 1610.01086
- Langer N, Norman CA, de Koter A, Vink JS, Cantiello M, Yoon SC (2007) Pair creation supernovae at low and high redshift. *Astron.Astrophys.* 475:L19–L23, DOI 10.1051/0004-6361:20078482, 0708.1970
- Leloudas G, Chatzopoulos E, Dilday B, Gorosabel J, Vinko J, Gallazzi A, Wheeler JC, Bassett B, Fischer JA, Frieman JA, Fynbo JPU, Goobar A, Jelínek M, Malesani D, Nichol RC, Nordin J, Östman L, Sako M, Schneider DP, Smith M, Sollerman J, Stritzinger MD, Thöne CC, de Ugarte Postigo A (2012) SN 2006oz: rise of a super-luminous supernova observed by the SDSS-II SN Survey. *Astron.Astrophys.* 541:A129, DOI 10.1051/0004-6361/201118498, 1201.5393

-
- Leloudas G, Patat F, Maund JR, Hsiao E, Malesani D, Schulze S, Contreras C, de Ugarte Postigo A, Sollerman J, Stritzinger MD, Taddia F, Wheeler JC, Gorosabel J (2015a) Polarimetry of the Superluminous Supernova LSQ14mo: No Evidence for Significant Deviations from Spherical Symmetry. *Astrophys.J.Lett.* 815:L10, DOI 10.1088/2041-8205/815/1/L10, 1511.04522
- Leloudas G, Schulze S, Krühler T, Gorosabel J, Christensen L, Mehner A, de Ugarte Postigo A, Amorín R, Thöne CC, Anderson JP, Bauer FE, Gallazzi A, Helminiak KG, Hjorth J, Ibar E, Malesani D, Morell N, Vinko J, Wheeler JC (2015b) Spectroscopy of superluminous supernova host galaxies. A preference of hydrogen-poor events for extreme emission line galaxies. *M.N.R.A.S.* 449:917–932, DOI 10.1093/mnras/stv320, 1409.8331
- Leloudas G, Fraser M, Stone NC, van Velzen S, Jonker PG, Arcavi I, Fremling C, Maund JR, Smartt SJ, Krühler T, Miller-Jones JCA, Vreeswijk PM, Gal-Yam A, Mazzali PA, De Cia A, Howell DA, Inserra C, Patat F, de Ugarte Postigo A, Yaron O, Ashall C, Bar I, Campbell H, Chen TW, Childress M, Elias-Rosa N, Harmanen J, Hosseinzadeh G, Johansson J, Kangas T, Kankare E, Kim S, Kuncarayakti H, Lyman J, Magee MR, Maguire K, Malesani D, Mattila S, McCully CV, Nicholl M, Prentice S, Romero-Cañizales C, Schulze S, Smith KW, Sollerman J, Sullivan M, Tucker BE, Valenti S, Wheeler JC, Young DR (2016) The superluminous transient ASASSN-15lh as a tidal disruption event from a Kerr black hole. *Nature Astronomy* 1:0002, DOI 10.1038/s41550-016-0002, 1609.02927
- Leloudas G, Maund JR, Gal-Yam A, Pursimo T, Hsiao E, Malesani D, Patat F, de Ugarte Postigo A, Sollerman J, Stritzinger MD, Wheeler JC (2017) Time-resolved Polarimetry of the Superluminous SN 2015bn with the Nordic Optical Telescope. *Astrophys.J.Lett.* 837:L14, DOI 10.3847/2041-8213/aa6157, 1702.05494
- Levan AJ, Read AM, Metzger BD, Wheatley PJ, Tanvir NR (2013) Superluminous X-Rays from a Superluminous Supernova. *Astrophys.J.* 771:136, DOI 10.1088/0004-637X/771/2/136, 1304.1173
- Liu LD, Wang SQ, Wang LJ, Dai ZG, Yu H, Peng ZK (2017a) A Monte Carlo Approach to Magnetar-powered Transients. I. Hydrogen-deficient Superluminous Supernovae. *Astrophys.J.* 842:26, DOI 10.3847/1538-4357/aa73d9, 1705.06047
- Liu YQ, Modjaz M, Bianco FB (2017b) Analyzing the Largest Spectroscopic Data Set of Hydrogen-poor Super-luminous Supernovae. *Astrophys.J.* 845:85, DOI 10.3847/1538-4357/aa7f74, 1612.07321
- Lunnan R, Chornock R, Berger E, Laskar T, Fong W, Rest A, Sanders NE, Challis PM, Drout MR, Foley RJ, Huber ME, Kirshner RP, Leibler C, Marion GH, McCrum M, Milisavljevic D, Narayan G, Scolnic D, Smartt SJ, Smith KW, Soderberg AM, Tonry JL, Burgett WS, Chambers KC, Flewelling H, Hodapp KW, Kaiser N, Magnier EA, Price PA, Wainscoat RJ (2014) Hydrogen-poor Superluminous Supernovae and Long-duration Gamma-Ray Bursts Have Similar Host Galaxies. *Astrophys.J.* 787:138, DOI 10.1088/0004-637X/787/2/138, 1311.0026
- Lunnan R, Chornock R, Berger E, Rest A, Fong W, Scolnic D, Jones DO, Soderberg AM, Challis PM, Drout MR, Foley RJ, Huber ME, Kirshner RP, Leibler C, Marion GH, McCrum M, Milisavljevic D, Narayan G, Sanders NE, Smartt SJ, Smith KW, Tonry JL, Burgett WS, Chambers KC, Flewelling H, Kudritzki RP, Wainscoat RJ, Waters C (2015) Zooming In on the Progenitors of Superluminous Supernovae With the HST. *Astrophys.J.* 804:90, DOI 10.1088/0004-637X/804/2/90, 1411.1060
- Lunnan R, Chornock R, Berger E, Milisavljevic D, Jones DO, Rest A, Fong W, Fransson C, Margutti R, Drout MR, Blanchard PK, Challis P, Cowperthwaite PS, Foley RJ, Kirshner RP, Morrell N, Riess AG, Roth KC, Scolnic D, Smartt SJ, Smith KW, Villar VA, Chambers KC, Draper PW, Huber ME, Kaiser N, Kudritzki RP, Magnier EA, Metcalfe N, Waters C (2016) PS1-14bj: A Hydrogen-poor Superluminous Supernova With a Long Rise and Slow Decay. *Astrophys.J.* 831:144, DOI 10.3847/0004-637X/831/2/144, 1605.05235

- Lunnan R, Chornock R, Berger E, Jones DO, Rest A, Czekala I, Dittmann J, Drout MR, Foley RJ, Fong W, Kirshner RP, Laskar T, Leibler CN, Margutti R, Milisavljevic D, Narayan G, Pan YC, Riess AG, Roth KC, Sanders NE, Scolnic D, Smartt SJ, Smith KW, Chambers KC, Draper PW, Flewelling H, Huber ME, Kaiser N, Kudritzki RP, Magnier EA, Metcalfe N, Wainscoat RJ, Waters C, Willman M (2018) Hydrogen-poor Superluminous Supernovae from the Pan-STARRS1 Medium Deep Survey. *Astrophys.J.* 852:81, DOI 10.3847/1538-4357/aa9f1a, 1708.01619
- Lyman JD, Bersier D, James PA, Mazzali PA, Eldridge JJ, Fraser M, Pian E (2016) Bolometric light curves and explosion parameters of 38 stripped-envelope core-collapse supernovae. *M.N.R.A.S.* 457:328–350, DOI 10.1093/mnras/stv2983, 1406.3667
- Madau P, Dickinson M (2014) Cosmic Star-Formation History. *Annu.Rev.Astron.Astrophys.* 52:415–486, DOI 10.1146/annurev-astro-081811-125615, 1403.0007
- Maeda K, Tanaka M, Nomoto K, Tominaga N, Kawabata K, Mazzali PA, Umeda H, Suzuki T, Hattori T (2007) The Unique Type Ib Supernova 2005bf at Nebular Phases: A Possible Birth Event of a Strongly Magnetized Neutron Star. *Astrophys.J.* 666:1069–1082, DOI 10.1086/520054, 0705.2713
- Margalit B, Metzger BD, Thompson TA, Nicholl M, Sukhbold T (2018) The GRB-SLSN connection: misaligned magnetars, weak jet emergence, and observational signatures. *M.N.R.A.S.* 475:2659–2674, DOI 10.1093/mnras/sty013, 1705.01103
- Margutti R, Chornock R, Metzger BD, Coppejans DL, Guidorzi C, Migliori G, Milisavljevic D, Berger E, Nicholl M, Zauderer BA, Lunnan R, Kamble A, Drout M, Modjaz M (2017) Results from a systematic survey of X-ray emission from Hydrogen-poor Superluminous Supernovae. *ArXiv e-prints* 1704.05865
- Matzner CD, McKee CF (1999) The Expulsion of Stellar Envelopes in Core-Collapse Supernovae. *Astrophys.J.* 510:379–403, DOI 10.1086/306571, astro-ph/9807046
- Mazzali PA, Sullivan M, Pian E, Greiner J, Kann DA (2016) Spectrum formation in superluminous supernovae (Type I). *M.N.R.A.S.* 458:3455–3465, DOI 10.1093/mnras/stw512, 1603.00388
- McCrum M, Smartt SJ, Rest A, Smith K, Kotak R, Rodney SA, Young DR, Chornock R, Berger E, Foley RJ, Fraser M, Wright D, Scolnic D, Tonry JL, Urata Y, Huang K, Pastorello A, Botticella MT, Valenti S, Mattila S, Kankare E, Farrow DJ, Huber ME, Stubbs CW, Kirshner RP, Bresolin F, Burgett WS, Chambers KC, Draper PW, Flewelling H, Jedicke R, Kaiser N, Magnier EA, Metcalfe N, Morgan JS, Price PA, Sweeney W, Wainscoat RJ, Waters C (2015) Selecting superluminous supernovae in faint galaxies from the first year of the Pan-STARRS1 Medium Deep Survey. *M.N.R.A.S.* 448:1206–1231, DOI 10.1093/mnras/stv034, 1402.1631
- Metzger BD, Vurm I, Hascoët R, Beloborodov AM (2014) Ionization break-out from millisecond pulsar wind nebulae: an X-ray probe of the origin of superluminous supernovae. *M.N.R.A.S.* 437:703–720, DOI 10.1093/mnras/stt1922, 1307.8115
- Miller AA, Chornock R, Perley DA, Ganeshalingam M, Li W, Butler NR, Bloom JS, Smith N, Modjaz M, Poznanski D, Filippenko AV, Griffith CV, Shiode JH, Silverman JM (2009) The Exceptionally Luminous Type II-Linear Supernova 2008es. *Astrophys.J.* 690:1303–1312, DOI 10.1088/0004-637X/690/2/1303, 0808.2193
- Miller AA, Smith N, Li W, Bloom JS, Chornock R, Filippenko AV, Prochaska JX (2010) New Observations of the Very Luminous Supernova 2006gy: Evidence for Echoes. *Astron.J.* 139:2218–2229, DOI 10.1088/0004-6256/139/6/2218, 0906.2201
- Moriya T, Tominaga N, Tanaka M, Maeda K, Nomoto K (2010) A Core-collapse Supernova Model for the Extremely Luminous Type Ic Supernova 2007bi: An Alternative to the Pair-instability Supernova Model. *Astrophys.J.Lett.* 717:L83–L86, DOI 10.1088/2041-8205/717/2/L83, 1004.2967

-
- Moriya TJ, Langer N (2015) Pulsations of red supergiant pair-instability supernova progenitors leading to extreme mass loss. *Astron.Astrophys.* 573:A18, DOI 10.1051/0004-6361/201424957, 1410.4557
- Moriya TJ, Maeda K (2012) A Dip after the Early Emission of Superluminous Supernovae: A Signature of Shock Breakout within Dense Circumstellar Media. *Astrophys.J.Lett.* 756:L22, DOI 10.1088/2041-8205/756/1/L22, 1203.1451
- Moriya TJ, Tominaga N (2012) Diversity of Luminous Supernovae from Non-steady Mass Loss. *Astrophys.J.* 747:118, DOI 10.1088/0004-637X/747/2/118, 1110.3807
- Moriya TJ, Blinnikov SI, Tominaga N, Yoshida N, Tanaka M, Maeda K, Nomoto K (2013a) Light-curve modelling of superluminous supernova 2006gy: collision between supernova ejecta and a dense circumstellar medium. *M.N.R.A.S.* 428:1020–1035, DOI 10.1093/mnras/sts075, 1204.6109
- Moriya TJ, Maeda K, Taddia F, Sollerman J, Blinnikov SI, Sorokina EI (2013b) An analytic bolometric light curve model of interaction-powered supernovae and its application to Type II_n supernovae. *M.N.R.A.S.* 435:1520–1535, DOI 10.1093/mnras/stt1392, 1307.2644
- Moriya TJ, Liu ZW, Mackey J, Chen TW, Langer N (2015) Revealing the binary origin of Type Ic superluminous supernovae through nebular hydrogen emission. *Astron.Astrophys.* 584:L5, DOI 10.1051/0004-6361/201527515, 1510.01621
- Moriya TJ, Metzger BD, Blinnikov SI (2016) Supernovae Powered by Magnetars that Transform into Black Holes. *Astrophys.J.* 833:64, DOI 10.3847/1538-4357/833/1/64, 1606.09316
- Moriya TJ, Chen TW, Langer N (2017a) Properties of Magnetars Mimicking ⁵⁶Ni-powered Light Curves in Type IC Superluminous Supernovae. *Astrophys.J.* 835:177, DOI 10.3847/1538-4357/835/2/177, 1612.06917
- Moriya TJ, Tanaka M, Morokuma T, Ohsuga K (2017b) Superluminous Transients at AGN Centers from Interaction between Black Hole Disk Winds and Broad-line Region Clouds. *Astrophys.J.Lett.* 843:L19, DOI 10.3847/2041-8213/aa7af3, 1706.06855
- Moriya TJ, Tanaka M, Yasuda N, Jiang Ja, Lee CH, Maeda K, Morokuma T, Nomoto K, Quimby RM, Suzuki N, Takahashi I, Tanaka M, Tominaga N, Yamaguchi M, Bernard SR, Cooke J, Curtin C, Galbany L, Gonzalez-Gaitan S, Pignata G, Pritchard T, Komiyama Y, Lupton RH (2018) First release of high-redshift superluminous supernovae from the Subaru HIGH-Z sUpernova CAmpaign (SHIZUCA). I. Photometric properties. *ArXiv e-prints* 1801.08240
- Nadyozhin DK (1994) The properties of Ni to Co to Fe decay. *Astrophys.J.Supp.* 92:527–531, DOI 10.1086/192008
- Neill JD, Sullivan M, Gal-Yam A, Quimby R, Ofek E, Wyder TK, Howell DA, Nugent P, Seibert M, Martin DC, Overzier R, Barlow TA, Foster K, Friedman PG, Morrissey P, Neff SG, Schiminovich D, Bianchi L, Donas J, Heckman TM, Lee YW, Madore BF, Milliard B, Rich RM, Szalay AS (2011) The Extreme Hosts of Extreme Supernovae. *Astrophys.J.* 727:15, DOI 10.1088/0004-637X/727/1/15, 1011.3512
- Nicholl M, Smartt SJ (2016) Seeing double: the frequency and detectability of double-peaked superluminous supernova light curves. *M.N.R.A.S.* 457:L79–L83, DOI 10.1093/mnrasl/slv210, 1511.03740
- Nicholl M, Smartt SJ, Jerkstrand A, Inserra C, Anderson JP, Baltay C, Benetti S, Chen TW, Elias-Rosa N, Feindt U, Fraser M, Gal-Yam A, Hadjiyska E, Howell DA, Kotak R, Lawrence A, Leloudas G, Margheim S, Mattila S, McCrum M, McKinnon R, Mead A, Nugent P, Rabinowitz D, Rest A, Smith KW, Sollerman J, Sullivan M, Taddia F, Valenti S, Walker ES, Young DR (2014) Superluminous supernovae from PESSTO. *M.N.R.A.S.* 444:2096–2113, DOI 10.1093/mnras/stu1579, 1405.1325
- Nicholl M, Smartt SJ, Jerkstrand A, Inserra C, Sim SA, Chen TW, Benetti S, Fraser M, Gal-Yam A, Kankare E, Maguire K, Smith K, Sullivan M, Valenti S, Young DR, Baltay C, Bauer FE, Baumont S, Bersier D, Botticella MT, Childress M, Deneffeld M, Della Valle M, Elias-Rosa N, Feindt U, Galbany L, Hadjiyska E, Le Guillou L, Leloudas G, Mazzali P, McKinnon R, Polshaw J, Ra-

- binowitz D, Rostami S, Scalzo R, Schmidt BP, Schulze S, Sollerman J, Taddia F, Yuan F (2015a) On the diversity of superluminous supernovae: ejected mass as the dominant factor. *M.N.R.A.S.* 452:3869–3893, DOI 10.1093/mnras/stv1522, 1503.03310
- Nicholl M, Smartt SJ, Jerkstrand A, Sim SA, Inserra C, Anderson JP, Baltay C, Benetti S, Chambers K, Chen TW, Elias-Rosa N, Feindt U, Flewelling HA, Fraser M, Gal-Yam A, Galbany L, Huber ME, Kangas T, Kankare E, Kotak R, Krühler T, Maguire K, McKinnon R, Rabinowitz D, Rostami S, Schulze S, Smith KW, Sullivan M, Tonry JL, Valenti S, Young DR (2015b) LSQ14bdq: A Type Ic Super-luminous Supernova with a Double-peaked Light Curve. *Astrophys.J.Lett.* 807:L18, DOI 10.1088/2041-8205/807/1/L18, 1505.01078
- Nicholl M, Berger E, Margutti R, Chornock R, Blanchard PK, Jerkstrand A, Smartt SJ, Arcavi I, Challis P, Chambers KC, Chen TW, Cowperthwaite PS, Gal-Yam A, Hosseinzadeh G, Howell DA, Inserra C, Kankare E, Magnier EA, Maguire K, Mazzali PA, McCully C, Milisavljevic D, Smith KW, Taubenberger S, Valenti S, Wainscoat RJ, Yaron O, Young DR (2016a) Superluminous Supernova SN 2015bn in the Nebular Phase: Evidence for the Engine-powered Explosion of a Stripped Massive Star. *Astrophys.J.Lett.* 828:L18, DOI 10.3847/2041-8205/828/2/L18, 1608.02995
- Nicholl M, Berger E, Smartt SJ, Margutti R, Kamble A, Alexander KD, Chen TW, Inserra C, Arcavi I, Blanchard PK, Cartier R, Chambers KC, Childress MJ, Chornock R, Cowperthwaite PS, Drout M, Flewelling HA, Fraser M, Gal-Yam A, Galbany L, Harmanen J, Holoien TWS, Hosseinzadeh G, Howell DA, Huber ME, Jerkstrand A, Kankare E, Kochanek CS, Lin ZY, Lunnan R, Magnier EA, Maguire K, McCully C, McDonald M, Metzger BD, Milisavljevic D, Mitra A, Reynolds T, Saario J, Shappee BJ, Smith KW, Valenti S, Villar VA, Waters C, Young DR (2016b) SN 2015BN: A Detailed Multi-wavelength View of a Nearby Superluminous Supernova. *Astrophys.J.* 826:39, DOI 10.3847/0004-637X/826/1/39, 1603.04748
- Nicholl M, Berger E, Margutti R, Blanchard PK, Guillochon J, Leja J, Chornock R (2017a) The Superluminous Supernova SN 2017egm in the Nearby Galaxy NGC 3191: A Metal-rich Environment Can Support a Typical SLSN Evolution. *Astrophys.J.Lett.* 845:L8, DOI 10.3847/2041-8213/aa82b1, 1706.08517
- Nicholl M, Guillochon J, Berger E (2017b) The Magnetar Model for Type I Superluminous Supernovae. I. Bayesian Analysis of the Full Multicolor Light-curve Sample with MOSFiT. *Astrophys.J.* 850:55, DOI 10.3847/1538-4357/aa9334, 1706.00825
- Ofek EO, Cameron PB, Kasliwal MM, Gal-Yam A, Rau A, Kulkarni SR, Frail DA, Chandra P, Cenko SB, Soderberg AM, Immler S (2007) SN 2006gy: An Extremely Luminous Supernova in the Galaxy NGC 1260. *Astrophys.J.Lett.* 659:L13–L16, DOI 10.1086/516749, astro-ph/0612408
- Ostriker JP, Gunn JE (1971) Do Pulsars Make Supernovae? *Astrophys.J.Lett.* 164:L95, DOI 10.1086/180699
- Ouyed R, Kostka M, Koning N, Leahy DA, Steffen W (2012) Quark nova imprint in the extreme supernova explosion SN 2006gy. *M.N.R.A.S.* 423:1652–1662, DOI 10.1111/j.1365-2966.2012.20986.x, 1010.5530
- Pan YC, Foley RJ, Smith M, Galbany L, D’Andrea CB, González-Gaitán S, Jarvis MJ, Kessler R, Kovacs E, Lidman CN R C, Papadopoulos A, Sako M, Sullivan M, Abbott TMC, Abdalla FB, Annis J, Bechtol K, Benoit-Lévy A, Brooks D, Buckley-Geer E, Burke DL, Carnero Rosell A, Carrasco Kind M, Carretero J, Castander FJ, Cunha CE, da Costa LN, Desai S, Diehl HT, Doel P, Eifler TF, Finley DA, Flaugher B, Frieman J, García-Bellido J, Goldstein DA, Gruen D, Gruendl RA, Gschwend J, Gutierrez G, James DJ, Kim AG, Krause E, Kuehn K, Kuropatkin N, Lahav O, Lima M, Maia MAG, March M, Marshall JL, Martini P, Miquel R, Nugent P, Plazas AA, Romer AK, Sanchez E, Scarpine V, Schubnell M, Sevilla-Noarbe I, Smith RC, Sobreira F, Suchyta E, Swanson MEC, Thomas RC, Walker AR, DES Collaboration (2017) DES15E2mlf: a spectroscopically confirmed superluminous supernova that exploded 3.5 Gyr after the big bang. *M.N.R.A.S.* 470:4241–4250, DOI 10.1093/mnras/stx1467,

- 1707.06649
- Pastorello A, Smartt SJ, Botticella MT, Maguire K, Fraser M, Smith K, Kotak R, Magill L, Valenti S, Young DR, Gezari S, Bresolin F, Kudritzki R, Howell DA, Rest A, Metcalfe N, Mattila S, Kankare E, Huang KY, Urata Y, Burgett WS, Chambers KC, Dombeck T, Flewelling H, Grav T, Heasley JN, Hodapp KW, Kaiser N, Luppino GA, Lupton RH, Magnier EA, Monet DG, Morgan JS, Onaka PM, Price PA, Rhoads PH, Siegmund WA, Stubbs CW, Sweeney WE, Tonry JL, Wainscoat RJ, Waterson MF, Waters C, Wynn-Williams CG (2010) Ultra-bright Optical Transients are Linked with Type Ic Supernovae. *Astrophys.J.Lett.* 724:L16–L21, DOI 10.1088/2041-8205/724/1/L16, 1008.2674
- Pastorello A, Wang XF, Ciabattari F, Bersier D, Mazzali PA, Gao X, Xu Z, Zhang JJ, Tokuoka S, Benetti S, Cappellaro E, Elias-Rosa N, Harutyunyan A, Huang F, Miluzio M, Mo J, Ochner P, Tartaglia L, Terreran G, Tomasella L, Turatto M (2016) Massive stars exploding in a He-rich circumstellar medium - IX. SN 2014av, and characterization of Type Ibn SNe. *M.N.R.A.S.* 456:853–869, DOI 10.1093/mnras/stv2634, 1509.09069
- Perley DA, Quimby RM, Yan L, Vreeswijk PM, De Cia A, Lunnan R, Gal-Yam A, Yaron O, Filippenko AV, Graham ML, Laher R, Nugent PE (2016) Host-galaxy Properties of 32 Low-redshift Superluminous Supernovae from the Palomar Transient Factory. *Astrophys.J.* 830:13, DOI 10.3847/0004-637X/830/1/13, 1604.08207
- Piro AL (2015) Using Double-peaked Supernova Light Curves to Study Extended Material. *Astrophys.J.Lett.* 808:L51, DOI 10.1088/2041-8205/808/2/L51, 1505.07103
- Porth O, Komissarov SS, Keppens R (2014) Rayleigh-Taylor instability in magnetohydrodynamic simulations of the Crab nebula. *M.N.R.A.S.* 443:547–558, DOI 10.1093/mnras/stu1082, 1405.4029
- Prajs S, Sullivan M, Smith M, Levan A, Karpenka NV, Edwards TDP, Walker CR, Wolf WM, Balland C, Carlberg R, Howell DA, Lidman C, Pain R, Pritchett C, Ruhlmann-Kleider V (2017) The volumetric rate of superluminous supernovae at $z \sim 1$. *M.N.R.A.S.* 464:3568–3579, DOI 10.1093/mnras/stw1942, 1605.05250
- Quimby RM (2006) The Texas Supernova Search. PhD thesis, The University of Texas at Austin
- Quimby RM, Kulkarni SR, Kasliwal MM, Gal-Yam A, Arcavi I, Sullivan M, Nugent P, Thomas R, Howell DA, Nakar E, Bildsten L, Theissen C, Law NM, Dekany R, Rahmer G, Hale D, Smith R, Ofek EO, Zolkower J, Velur V, Walters R, Henning J, Bui K, McKenna D, Poznanski D, Cenko SB, Levitan D (2011) Hydrogen-poor superluminous stellar explosions. *Nature* 474:487–489, DOI 10.1038/nature10095, 0910.0059
- Quimby RM, Yuan F, Akerlof C, Wheeler JC (2013) Rates of superluminous supernovae at $z \sim 0.2$. *M.N.R.A.S.* 431:912–922, DOI 10.1093/mnras/stt213, 1302.0911
- Quimby RM, De Cia A, Gal-Yam A, Leloudas G, Lunnan R, Perley DA, Vreeswijk PM, Yan L, Bloom JS, Cenko SB, Cooke J, Ellis R, Filippenko AV, Kasliwal MM, Kleiser IKW, Kulkarni SR, Matheson T, Nugent PE, Pan YC, Silverman JM, Sternberg A, Sullivan M, Yaron O (2018) Spectra of Hydrogen-Poor Superluminous Supernovae from the Palomar Transient Factory. *ArXiv e-prints* 1802.07820
- Rakavy G, Shaviv G (1967) Instabilities in Highly Evolved Stellar Models. *Astrophys.J.* 148:803, DOI 10.1086/149204
- Renault-Tinacci N, Kotera K, Neronov A, Ando S (2017) Search for gamma-ray emission from super-luminous supernovae with the Fermi-LAT. *ArXiv e-prints* 1708.08971
- Rest A, Foley RJ, Gezari S, Narayan G, Draine B, Olsen K, Huber ME, Matheson T, Garg A, Welch DL, Becker AC, Challis P, Clocchiatti A, Cook KH, Damke G, Meixner M, Miknaitis G, Minniti D, Morelli L, Nikolaev S, Pignata G, Prieto JL, Smith RC, Stubbs C, Suntzeff NB, Walker AR, Wood-Vasey WM, Zenteno A, Wyrzykowski L, Udalski A, Szymański MK, Kubiak M, Pietrzyński G, Soszyński I, Szewczyk O, Ulaczyk K, Poleski R (2011) Pushing the Bound-

- aries of Conventional Core-collapse Supernovae: The Extremely Energetic Supernova SN 2003ma. *Astrophys.J.* 729:88, DOI 10.1088/0004-637X/729/2/88, 0911.2002
- Reynolds SP (2016) *Dynamical Evolution and Radiative Processes of Supernova Remnants*, Springer International Publishing, Cham, pp 1–24. DOI 10.1007/978-3-319-20794-0_89-1, URL https://doi.org/10.1007/978-3-319-20794-0_89-1
- Richardson D, Jenkins RL III, Wright J, Maddox L (2014) Absolute-magnitude Distributions of Supernovae. *Astron.J.* 147:118, DOI 10.1088/0004-6256/147/5/118, 1403.5755
- Roy R, Sollerman J, Silverman JM, Pastorello A, Fransson C, Drake A, Taddia F, Fremling C, Kankare E, Kumar B, Cappellaro E, Bose S, Benetti S, Filippenko AV, Valenti S, Nyholm A, Ergon M, Sutaria F, Kumar B, Pandey SB, Nicholl M, Garcia-Álvarez D, Tomasella L, Karamehmetoglu E, Migotto K (2016) SN 2012aa: A transient between Type Ibc core-collapse and superluminous supernovae. *Astron.Astrophys.* 596:A67, DOI 10.1051/0004-6361/201527947, 1607.00924
- Scannapieco E, Madau P, Woosley S, Heger A, Ferrara A (2005) The Detectability of Pair-Production Supernovae at $z \lesssim 6$. *Astrophys.J.* 633:1031–1041, DOI 10.1086/444450, astro-ph/0507182
- Schulze S, Krühler T, Leloudas G, Gorosabel J, Mehner A, Buchner J, Kim S, Ibar E, Amorín R, Herrero-Illana R, Anderson JP, Bauer FE, Christensen L, de Pasquale M, de Ugarte Postigo A, Gallazzi A, Hjorth J, Morrell N, Malesani D, Sparre M, Stalder B, Stark AA, Thöne CC, Wheeler JC (2018) Cosmic evolution and metal aversion in superluminous supernova host galaxies. *M.N.R.A.S.* 473:1258–1285, DOI 10.1093/mnras/stx2352, 1612.05978
- Scovaccicchi D, Nichol RC, Bacon D, Sullivan M, Prajs S (2016) Cosmology with superluminous supernovae. *M.N.R.A.S.* 456:1700–1707, DOI 10.1093/mnras/stv2752, 1511.06670
- Smith M, Sullivan M, D’Andrea CB, Castander FJ, Casas R, Prajs S, Papadopoulos A, Nichol RC, Karpenka NV, Bernard SR, Brown P, Cartier R, Cooke J, Curtin C, Davis TM, Finley DA, Foley RJ, Gal-Yam A, Goldstein DA, González-Gaitán S, Gupta RR, Howell DA, Inserra C, Kessler R, Lidman C, Marriner J, Nugent P, Pritchard TA, Sako M, Smartt S, Smith RC, Spinka H, Thomas RC, Wolf RC, Zenteno A, Abbott TMC, Benoit-Lévy A, Bertin E, Brooks D, Buckley-Geer E, Carnero Rosell A, Carrasco Kind M, Carretero J, Croce M, Cunha CE, da Costa LN, Desai S, Diehl HT, Doel P, Estrada J, Evrard AE, Flaughner B, Fosalba P, Frieman J, Gerdes DW, Gruen D, Gruendl RA, James DJ, Kuehn K, Kuropatkin N, Lahav O, Li TS, Marshall JL, Martini P, Miller CJ, Miquel R, Nord B, Ogando R, Plazas AA, Reil K, Romer AK, Roodman A, Rykoff ES, Sanchez E, Scarpine V, Schubnell M, Sevilla-Noarbe I, Soares-Santos M, Sobreira F, Suchyta E, Swanson MEC, Tarle G, Walker AR, Wester W, DES Collaboration (2016) DES14X3taz: A Type I Superluminous Supernova Showing a Luminous, Rapidly Cooling Initial Pre-peak Bump. *Astrophys.J.Lett.* 818:L8, DOI 10.3847/2041-8205/818/1/L8, 1512.06043
- Smith M, Sullivan M, Nichol RC, Galbany L, D’Andrea CB, Inserra C, Lidman C, Rest A, Schirmer M, Filippenko AV, Zheng W, Cenko SB, Angus CR, Brown PJ, Davis TM, Finley DA, Foley RJ, González-Gaitán S, Gutiérrez CP, Kessler R, Kuhlmann S, Marriner J, Möller A, Nugent PE, Prajs S, Thomas R, Wolf R, Zenteno A, Abbott TMC, Abdalla FB, Allam S, Annis J, Bechtol K, Benoit-Lévy A, Bertin E, Brooks D, Burke DL, Carnero Rosell A, Carrasco Kind M, Carretero J, Castander FJ, Croce M, Cunha CE, da Costa LN, Davis C, Desai S, Diehl HT, Doel P, Eifler TF, Flaughner B, Fosalba P, Frieman J, García-Bellido J, Gaztanaga E, Gerdes DW, Goldstein DA, Gruen D, Gruendl RA, Gschwend J, Gutierrez G, Honscheid K, James DJ, Johnson MWG, Kuehn K, Kuropatkin N, Li TS, Lima M, Maia MAG, Marshall JL, Martini P, Menanteau F, Miller CJ, Miquel R, Ogando RLC, Petravick D, Plazas AA, Romer AK, Rykoff ES, Sako M, Sanchez E, Scarpine V, Schindler R, Schubnell M, Sevilla-Noarbe I, Smith RC, Soares-Santos M, Sobreira F, Suchyta E, Swanson MEC,

- Tarle G, Walker AR, The DES Collaboration (2018) Studying the Ultraviolet Spectrum of the First Spectroscopically Confirmed Supernova at Redshift Two. *Astrophys.J.* 854:37, DOI 10.3847/1538-4357/aaa126, 1712.04535
- Smith N, Owocki SP (2006) On the Role of Continuum-driven Eruptions in the Evolution of Very Massive Stars and Population III Stars. *Astrophys.J.Lett.* 645:L45–L48, DOI 10.1086/506523, astro-ph/0606174
- Smith N, Li W, Foley RJ, Wheeler JC, Pooley D, Chornock R, Filippenko AV, Silverman JM, Quimby R, Bloom JS, Hansen C (2007) SN 2006gy: Discovery of the Most Luminous Supernova Ever Recorded, Powered by the Death of an Extremely Massive Star like η Carinae. *Astrophys.J.* 666:1116–1128, DOI 10.1086/519949, astro-ph/0612617
- Smith N, Chornock R, Li W, Ganeshalingam M, Silverman JM, Foley RJ, Filippenko AV, Barth AJ (2008a) SN 2006tf: Precursor Eruptions and the Optically Thick Regime of Extremely Luminous Type II_n Supernovae. *Astrophys.J.* 686:467–484, DOI 10.1086/591021, 0804.0042
- Smith N, Foley RJ, Bloom JS, Li W, Filippenko AV, Gavazzi R, Ghez A, Konopacky Q, Malkan MA, Marshall PJ, Pooley D, Treu T, Woo JH (2008b) Late-Time Observations of SN 2006gy: Still Going Strong. *Astrophys.J.* 686:485–491, DOI 10.1086/590141, 0802.1743
- Smith N, Chornock R, Silverman JM, Filippenko AV, Foley RJ (2010) Spectral Evolution of the Extraordinary Type II_n Supernova 2006gy. *Astrophys.J.* 709:856–883, DOI 10.1088/0004-637X/709/2/856, 0906.2200
- Smith N, Li W, Silverman JM, Ganeshalingam M, Filippenko AV (2011) Luminous blue variable eruptions and related transients: diversity of progenitors and outburst properties. *M.N.R.A.S.* 415:773–810, DOI 10.1111/j.1365-2966.2011.18763.x, 1010.3718
- Soderberg AM, Kulkarni SR, Nakar E, Berger E, Cameron PB, Fox DB, Frail D, Gal-Yam A, Sari R, Cenko SB, Kasliwal M, Chevalier RA, Piran T, Price PA, Schmidt BP, Pooley G, Moon DS, Penprase BE, Ofek E, Rau A, Gehrels N, Nousek JA, Burrows DN, Persson SE, McCarthy PJ (2006) Relativistic ejecta from X-ray flash XRF 060218 and the rate of cosmic explosions. *Nature* 442:1014–1017, DOI 10.1038/nature05087, astro-ph/0604389
- Soker N, Gilkis A (2017) Magnetar-powered Superluminous Supernovae Must First Be Exploded by Jets. *Astrophys.J.* 851:95, DOI 10.3847/1538-4357/aa9c83, 1708.08356
- Sorokina E, Blinnikov S, Nomoto K, Quimby R, Tolstov A (2016) Type I Superluminous Supernovae as Explosions inside Non-hydrogen Circumstellar Envelopes. *Astrophys.J.* 829:17, DOI 10.3847/0004-637X/829/1/17, 1510.00834
- Spitkovsky A (2006) Time-dependent Force-free Pulsar Magnetospheres: Axisymmetric and Oblique Rotators. *Astrophys.J.Lett.* 648:L51–L54, DOI 10.1086/507518, astro-ph/0603147
- Suzuki A, Maeda K (2017) Supernova ejecta with a relativistic wind from a central compact object: a unified picture for extraordinary supernovae. *M.N.R.A.S.* 466:2633–2657, DOI 10.1093/mnras/stw3259, 1612.03911
- Taddia F, Sollerman J, Leloudas G, Stritzinger MD, Valenti S, Galbany L, Kessler R, Schneider DP, Wheeler JC (2015) Early-time light curves of Type Ib/c supernovae from the SDSS-II Supernova Survey. *Astron.Astrophys.* 574:A60, DOI 10.1051/0004-6361/201423915, 1408.4084
- Takahashi K, Yoshida T, Umeda H, Sumiyoshi K, Yamada S (2016) Exact and approximate expressions of energy generation rates and their impact on the explosion properties of pair instability supernovae. *M.N.R.A.S.* 456:1320–1331, DOI 10.1093/mnras/stv2649, 1511.03040
- Terreran G, Pumo ML, Chen TW, Moriya TJ, Taddia F, Dessart L, Zampieri L, Smartt SJ, Benetti S, Inserra C, Cappellaro E, Nicholl M, Fraser M, Wyrzykowski L, Udalski A, Howell DA, McCully C, Valenti S, Dimitriadis G, Maguire K, Sullivan M, Smith KW, Yaron O, Young DR, Anderson JP, Della Valle M, Elias-Rosa N, Gal-Yam A, Jerkstrand A, Kankare E, Pastorello A, Sollerman J, Turatto M, Kostrzewa-Rutkowska Z, Kozłowski S, Mróz P, Pawlak M, Pietrukowicz P, Poleski R, Skowron D, Skowron J, Soszyński

- I, Szymański MK, Ulaczyk K (2017) Hydrogen-rich supernovae beyond the neutrino-driven core-collapse paradigm. *Nature Astronomy* 1:713–720, DOI 10.1038/s41550-017-0228-8, 1709.10475
- Thöne CC, de Ugarte Postigo A, García-Benito R, Leloudas G, Schulze S, Amorín R (2015) A young stellar environment for the superluminous supernova PTF12dam. *M.N.R.A.S.* 451:L65–L69, DOI 10.1093/mnras/slv051, 1411.1104
- Tolstov A, Blinnikov S, Nagataki S, Nomoto K (2015) Shock Wave Structure in Astrophysical Flows with an Account of Photon Transfer. *Astrophys.J.* 811:47, DOI 10.1088/0004-637X/811/1/47, 1412.1434
- Tolstov A, Nomoto K, Blinnikov S, Sorokina E, Quimby R, Baklanov P (2017a) Pulsational Pair-instability Model for Superluminous Supernova PTF12dam: Interaction and Radioactive Decay. *Astrophys.J.* 835:266, DOI 10.3847/1538-4357/835/2/266, 1612.01634
- Tolstov A, Zhiglo A, Nomoto K, Sorokina E, Kozyreva A, Blinnikov S (2017b) Ultraviolet Light Curves of Gaia16apd in Superluminous Supernova Models. *Astrophys.J.Lett.* 845:L2, DOI 10.3847/2041-8213/aa808e, 1707.05746
- Umeda H, Nomoto K (2008) How Much ^{56}Ni Can Be Produced in Core-Collapse Supernovae? Evolution and Explosions of 30–100 M Stars. *Astrophys.J.* 673:1014–1022, DOI 10.1086/524767, 0707.2598
- Vink JS (ed) (2015) Very Massive Stars in the Local Universe, *Astrophysics and Space Science Library*, vol 412, DOI 10.1007/978-3-319-09596-7, 1406.4836
- Vlasis A, Dessart L, Audit E (2016) Two-dimensional radiation hydrodynamics simulations of superluminous interacting supernovae of Type II. *M.N.R.A.S.* 458:1253–1266, DOI 10.1093/mnras/stw410, 1602.05864
- Vreeswijk PM, Savaglio S, Gal-Yam A, De Cia A, Quimby RM, Sullivan M, Cenko SB, Perley DA, Filippenko AV, Clubb KI, Taddia F, Sollerman J, Leloudas G, Arcavi I, Rubin A, Kasliwal MM, Cao Y, Yaron O, Tal D, Ofek EO, Capone J, Kutyrev AS, Toy V, Nugent PE, Laher R, Surace J, Kulkarni SR (2014) The Hydrogen-poor Superluminous Supernova iPTF 13ajg and its Host Galaxy in Absorption and Emission. *Astrophys.J.* 797:24, DOI 10.1088/0004-637X/797/1/24, 1409.8287
- Vreeswijk PM, Leloudas G, Gal-Yam A, De Cia A, Perley DA, Quimby RM, Waldman R, Sullivan M, Yan L, Ofek EO, Fremling C, Taddia F, Sollerman J, Valenti S, Arcavi I, Howell DA, Filippenko AV, Cenko SB, Yaron O, Kasliwal MM, Cao Y, Ben-Ami S, Horesh A, Rubin A, Lunnan R, Nugent PE, Laher R, Rebbapragada UD, Woźniak P, Kulkarni SR (2017) On the Early-time Excess Emission in Hydrogen-poor Superluminous Supernovae. *Astrophys.J.* 835:58, DOI 10.3847/1538-4357/835/1/58, 1609.08145
- Wang SQ, Wang LJ, Dai ZG, Wu XF (2015) Superluminous Supernovae Powered by Magnetars: Late-time Light Curves and Hard Emission Leakage. *Astrophys.J.* 799:107, DOI 10.1088/0004-637X/799/1/107, 1411.5126
- Weaver TA (1976) The structure of supernova shock waves. *Astrophys.J.Supp.* 32:233–282, DOI 10.1086/190398
- Wei JJ, Wu XF, Melia F (2015) Testing Cosmological Models with Type Ic Superluminous Supernovae. *Astron.J.* 149:165, DOI 10.1088/0004-6256/149/5/165, 1503.06378
- Whalen DJ, Smidt J, Heger A, Hirschi R, Yusof N, Even W, Fryer CL, Stiavelli M, Chen KJ, Joggerst CC (2014) Pair-instability Supernovae in the Local Universe. *Astrophys.J.* 797:9, DOI 10.1088/0004-637X/797/1/9, 1312.5360
- Wheeler JC, Chatzopoulos E, Vinkó J, Tuminello R (2017) Circumstellar Interaction Models for the Bolometric Light Curve of Type I Superluminous SN 2017egm. *Astrophys.J.Lett.* 851:L14, DOI 10.3847/2041-8213/aa9d84, 1710.04994
- Wosley SE (2010) Bright Supernovae from Magnetar Birth. *Astrophys.J.Lett.* 719:L204–L207, DOI 10.1088/2041-8205/719/2/L204, 0911.0698
- Wosley SE (2017) Pulsational Pair-instability Supernovae. *Astrophys.J.* 836:244, DOI 10.3847/1538-4357/836/2/244, 1608.08939
- Wosley SE, Blinnikov S, Heger A (2007) Pulsational pair instability as an explanation for the most luminous supernovae. *Nature* 450:390–392, DOI

-
- 10.1038/nature06333, 0710.3314
- Yan L, Quimby R, Ofek E, Gal-Yam A, Mazzali P, Perley D, Vreeswijk PM, Leloudas G, de Cia A, Masci F, Cenko SB, Cao Y, Kulkarni SR, Nugent PE, Rebbapragada UD, Woźniak PR, Yaron O (2015) Detection of Broad H α Emission Lines in the Late-time Spectra of a Hydrogen-poor Superluminous Supernova. *Astrophys.J.* 814:108, DOI 10.1088/0004-637X/814/2/108, 1508.04420
- Yan L, Lunnan R, Perley DA, Gal-Yam A, Yaron O, Roy R, Quimby R, Sollerman J, Fremling C, Leloudas G, Cenko SB, Vreeswijk P, Graham ML, Howell DA, De Cia A, Ofek EO, Nugent P, Kulkarni SR, Hosseinzadeh G, Masci F, McCully C, Rebbapragada UD, Woźniak P (2017a) Hydrogen-poor Superluminous Supernovae with Late-time H α Emission: Three Events From the Intermediate Palomar Transient Factory. *Astrophys.J.* 848:6, DOI 10.3847/1538-4357/aa8993, 1704.05061
- Yan L, Perley DA, De Cia A, Quimby R, Lunnan R, Rubin KHR, Brown PJ (2017b) Far-UV HST Spectroscopy of An Unusual Hydrogen Poor Superluminous Supernova: SN2017egm. ArXiv e-prints 1711.01534
- Yan L, Quimby R, Gal-Yam A, Brown P, Blagorodnova N, Ofek EO, Lunnan R, Cooke J, Cenko SB, Jencson J, Kasliwal M (2017c) Far-ultraviolet to Near-infrared Spectroscopy of a Nearby Hydrogen-poor Superluminous Supernova Gaia16apd. *Astrophys.J.* 840:57, DOI 10.3847/1538-4357/aa6b02, 1611.02782
- Yaron O, Gal-Yam A (2012) WISEREP - An Interactive Supernova Data Repository. *Pub.Astr.Soc.Pacific* 124:668, DOI 10.1086/666656, 1204.1891
- Yoon SC, Dierks A, Langer N (2012) Evolution of massive Population III stars with rotation and magnetic fields. *Astron.Astrophys.* 542:A113, DOI 10.1051/0004-6361/201117769, 1201.2364
- Young DR, Smartt SJ, Valenti S, Pastorello A, Benetti S, Benn CR, Bersier D, Botticella MT, Corradi RLM, Harutyunyan AH, Hrudkova M, Hunter I, Mattila S, de Mooij EJW, Navasardyan H, Snellen IAG, Tanvir NR, Zampieri L (2010) Two type Ic supernovae in low-metallicity, dwarf galaxies: diversity of explosions. *Astron.Astrophys.* 512:A70, DOI 10.1051/0004-6361/200913004, 0910.2248
- Yu YW, Li SZ (2017) A possible relation between flare activity in super-luminous supernovae and gamma-ray bursts. *M.N.R.A.S.* 470:197–201, DOI 10.1093/mnras/stx1028, 1607.00626
- Yu YW, Zhu JP, Li SZ, Lü HJ, Zou YC (2017) A Statistical Study of Superluminous Supernovae Using the Magnetar Engine Model and Implications for Their Connection with Gamma-Ray Bursts and Hypernovae. *Astrophys.J.* 840:12, DOI 10.3847/1538-4357/aa6c27, 1704.01682
- Yusof N, Hirschi R, Meynet G, Crowther PA, Ekström S, Frischknecht U, Georgy C, Abu Kassim H, Schnurr O (2013) Evolution and fate of very massive stars. *M.N.R.A.S.* 433:1114–1132, DOI 10.1093/mnras/stt794, 1305.2099
- Zhang T, Wang X, Wu C, Chen J, Chen J, Liu Q, Huang F, Liang J, Zhao X, Lin L, Wang M, Dennefeld M, Zhang J, Zhai M, Wu H, Fan Z, Zou H, Zhou X, Ma J (2012) Type II_n Supernova SN 2010jl: Optical Observations for over 500 Days after Explosion. *Astron.J.* 144:131, DOI 10.1088/0004-6256/144/5/131, 1208.6078